Legacy of Ian Balitsky: the first 70 years


The BFKL Equation


- All of our high-energy QCD field originated from the BFKL equation (1977-78).

The Pomeranchuk singularity in nonabelian gauge theories

É. A. Kuraev, L. N. Lipatov, and V. S. Fadin

Institute for Nuclear Physics, Siberian Division, USSR Academy of Sciences, Novosibirsk
(Submitted June 7, 1976)
Zh. Eksp. Teor. Fiz. **72**, 377–389 (February 1977)

An integral equation is derived for the t-channel partial wave amplitudes in the investigation of the multi-Regge form of the $2\to 2+n$ amplitude. For a t-channel state with isospin $T=1$ the solution of this equation is a Regge pole. The analytic properties of the isospin $T=0$, 2 partial wave amplitudes are investigated near the threshold for the production of two or three particles. It is shown that in the j-plane there are moving poles and cuts. For the $T=0$ vacuum channel it was found that the partial wave amplitude has a fixed square-root type branch point to the right of $j=1$.

PACS numbers: 12.40.Mm, 11.80.Et

The Pomeranchuk singularity in quantum chromodynamics

Ya. Ya. Balitskiĭ and L. N. Lipatov

Leningrad Nuclear Physics Institute, Academy of Sciences of the USSR
(Submitted 2 August 1978)
Yad. Fiz. **28**, 1597–1611 (December 1978)

The high-energy asymptotic form of the scattering amplitude of colorless particles in quantum chromodynamics is obtained in the leading logarithmic approximation. It is argued that such a calculation is justified for the amplitudes of scattering in which charmed quarks participate. The cross section for formation of two pairs of charmed quarks in $\gamma\gamma$ collisions is found in explicit form.

PACS numbers: 12.40.Bb

- Each paper has about 4,000 citations.
- This was Ian's PhD thesis.

$$\frac{\partial G\left(\vec{l}_\perp,\vec{l}'_\perp,Y\right)}{\partial Y}=\frac{\alpha_s N_c}{\pi^2}\int\frac{d^2q_\perp}{(\vec{l}_\perp-\vec{q}_\perp)^2}\left[G\left(\vec{q}_\perp,\vec{l}'_\perp,Y\right)-\frac{l_\perp^2}{2\,q_\perp^2}G\left(\vec{l}_\perp,\vec{l}'_\perp,Y\right)\right]$$

Collaboration with Volodya Braun

In late 1980s and in the 1990s,
Ian collaborated with Volodya Braun.

This was a productive collaboration, with many interesting and important results.

Those include works on instanton contributions to high energy scattering and on instanton valleys.

Collaboration with Volodya Braun

- Together, Ian and Volodya were the first to derive DGLAP evolution equation by running the evolution from the projectile, using the background field method.

- This paper has close to 700 citations and is becoming very topical these days, with the current push to unify small- and large-x evolution.

Nuclear Physics B311 (1988/89) 541–584
North-Holland, Amsterdam

EVOLUTION EQUATIONS FOR QCD STRING OPERATORS

I.I. BALITSKY and V.M. BRAUN

Leningrad Nuclear Physics Institute, Gatchina, Leningrad 188350, USR

Received 6 January 1988

It is shown that all of the usual programs for the operator expansion can be performed in terms of string operators on the light cone; namely, the separation of contributions from large and small distances, the study of higher twist corrections and the renormalization group analysis. Evolution equations for the leading-twist QCD string operators such as $\bar{\psi}(x)P\exp(ig\int_C A_\mu \mathrm{d}x_\mu)\psi(0)$ are studied in the coordinate space, which has an advantage of preserving explicitly the Lorentz and (in one-loop) conformal invariance of the theory. The solution is found, relating the two string operators in different normalization points. Its short-distance expansion reproduces conventional results for the summation of leading logs in deep inelastic scattering and evolution of hadron wave functions. The light-cone expansion of string operators provides an effective covariant technique for a separation of higher twist effects. As an illustration we calculate the twist-three and twist-four corrections for the deep inelastic scattering and confirm in this way the recent results on the renormalization of twist-three operators.

The BK Equation

- In 1996, Ian derived a high-energy evolution equation for Wilson lines.
- Buried deep inside the 57-page paper, the equation went initially unnoticed.
- In 1998, I invited Ian to give a seminar at the U. of Minnesota. His operator language was so alien to me, I did not understand the main result.

MIT-CTP-2470

hep-ph/9509348

September1995

OPERATOR EXPANSION FOR HIGH-ENERGY SCATTERING

I.BALITSKY*

Center for Theoretical Physics, Laboratory for Nuclear Science
Department of Physics, MIT, Cambridge 02139

ABSTRACT

I demonstrate that the leading logarithms for high-energy scattering can be obtained as a result of evolution of the nonlocal operators - straight-line ordered gauge factors - with respect to the slope of the straight line.

The BK Equation

- I derived the same equation in 1999, using a diagrammatic approach. I did not know it was the same equation until Alex pointed it out in Ian's paper some months later.

- Ian's paper now has over 2,000 citations.

$$\partial_Y N_{\mathbf{x}_0,\mathbf{x}_1}(Y) = \frac{\alpha_s\, N_c}{2\,\pi^2} \int d^2x_2\, \frac{x_{01}^2}{x_{02}^2\, x_{21}^2}\, [N_{\mathbf{x}_0,\mathbf{x}_2}(Y) + N_{\mathbf{x}_2,\mathbf{x}_1}(Y) - N_{\mathbf{x}_0,\mathbf{x}_1}(Y) - N_{\mathbf{x}_0,\mathbf{x}_2}(Y)\, N_{\mathbf{x}_2,\mathbf{x}_1}(Y)]$$

rcBK

Running coupling corrections to BK evolution were independently calculated by Ian and by Heribert Weigert and myself in 2006.

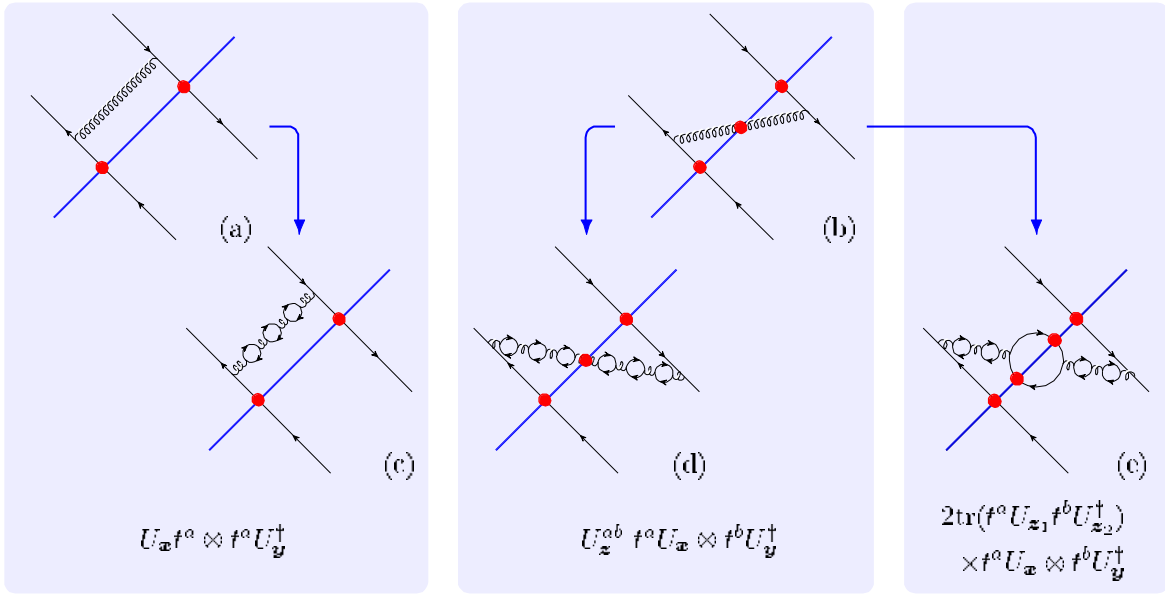

There was an issue of extracting the UV-divergent part of the right-most diagram. Ian and Heribert&me did this in two different ways. Hence, we obtained two different rcBK prescriptions.

Ian's approach turned out to be more accurate, in the sense of better capturing the contribution of the entire diagram in the rc subtraction procedure.

The NLO BK Equation

- Ian and Giovanni Chirilli calculated NLO BK equation in 2007.
- This is a very hard calculation. The result is the state-of-the-art in the field.
- The paper has over 400 citations.

$$\frac{d}{d\eta}N(x,y)=\frac{\alpha_s N_c}{2\pi^2}\int d^2z\frac{(x-y)^2}{X^2Y^2}\left\{1+\frac{\alpha_s N_c}{4\pi}\left[\frac{11}{3}\ln(x-y)^2\mu^2-\frac{11}{3}\frac{X^2-Y^2}{(x-y)^2}\ln\frac{X^2}{Y^2}+\frac{67}{9}-\frac{\pi^2}{3}-2\ln\frac{X^2}{(x-y)^2}\ln\frac{Y^2}{(x-y)^2}\right]\right\}$$
$$\times[N(x,z)+N(z,y)-N(x,y)-N(x,z)N(z,y)]$$
$$+\frac{\alpha_s^2N_c^2}{8\pi^4}\int d^2zd^2z'\left\{-\frac{2}{(z-z')^4}+\left[\frac{X^2Y'^2+X'^2Y^2-4(x-y)^2(z-z')^2}{(z-z')^4(X^2Y'^2-X'^2Y^2)}+\frac{(x-y)^4}{X^2Y'^2(X^2Y'^2-X'^2Y^2)}\right.\right.$$
$$\left.\left.+\frac{(x-y)^2}{X^2Y'^2(z-z')^2}\right]\ln\frac{X^2Y'^2}{X'^2Y^2}\right\}[N(z,z')-N(x,z)N(z,z')-N(z,z')N(z',y)-N(x,z)N(z',y)+N(x,z)N(z,y)$$
$$+N(x,z)N(z,z')N(z',y)]. \qquad (136)$$

Diagrams with 2 gluons interaction

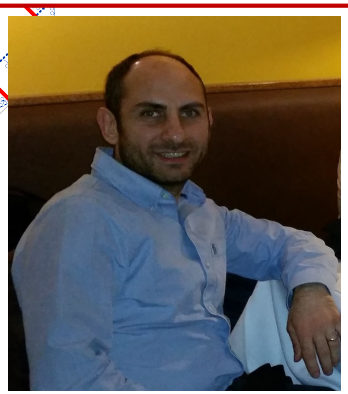

JLAB-THY-07-741

NLO evolution of color dipoles

Ian Balitsky and Giovanni A. Chirilli
Physics Dept., ODU, Norfolk VA 23529,
and
Theory Group, Jlab, 12000 Jefferson Ave,
Newport News, VA 23606
(Dated: October 24, 2018)

The small-x deep inelastic scattering in the saturation region is governed by the non-linear evolution of Wilson-line operators. In the leading logarithmic approximation it is given by the BK equation for the evolution of color dipoles. In the next-to-leading order the BK equation gets contributions from quark and gluon loops as well as from the tree gluon diagrams with quadratic and cubic nonlinearities. We calculate the gluon contribution to small-x evolution of Wilson lines (the quark part was obtained earlier).

PACS numbers: 12.38.Bx, 12.38.Cy

Unifying small- and large-x evolution

- In 2015, together with Andrey Tarasov, Ian formulated a new evolution equation, unifying DGLAP, CSS and small-x evolution.
- This is a hot topic these days in many meetings, including this one.

Prepared for submission to JHEP JLAB-THY-15-2040

Rapidity evolution of gluon TMD from low to moderate x

I. Balitsky* **and A. Tarasov†**

* *Physics Dept., Old Dominion University, Norfolk VA 23529,USA and Theory Group, JLAB, 12000 Jefferson Ave, Newport News, VA 23606,USA*

† *Theory Group, JLAB, 12000 Jefferson Ave, Newport News, VA 23606,USA*

E-mail: balitsky@jlab.org, atarasov@jlab.org

Abstract: We study how the rapidity evolution of gluon transverse momentum dependent distribution changes from nonlinear evolution at small $x \ll 1$ to linear evolution at moderate $x \sim 1$.

(See also 1905.09144 [hep-ph] and 2205.03119 [hep-ph] with Giovanni.)

Operator treatment

- While I never directly collaborated with Ian, he has greatly influenced my work over the last 25+ years.
- I even took up scuba diving, in part being inspired by his example.
- Over the last 10+ years, my group and I have been working on sub-eikonal small-x evolution, particularly for helicity (see my talk later).
- I first tried doing it using the diagrammatic (LCPT) approach. For the first 3-4 years, Ian would ask me every time he would see me: "*what are the corresponding operators?*"
- In the end, Ian was right, and it turned out easier to tackle the problem in the operator formalism. It helped me find an earlier mistake in our approach. We now refer to the blend of LCPT and the background field method that Ian uses as the **Light-Cone Operator Treatment (LCOT).**

Happy Birthday, Ian!

Probing small-x helicity distributions in particle production at RHIC and EIC

YURI KOVCHEGOV

THE OHIO STATE UNIVERSITY

Credits

- Based on work done with Dan Pitonyak and Matt Sievert (2015-2018, 2021-present), Florian Cougoulic (2019-present), Gabe Santiago (2020-present), Josh Tawabutr (2020-present), Andrey Tarasov (2021-present), Daniel Adamiak, Wally Melnitchouk, Nobuo Sato (2021-present), Jeremy Borden (2023-present), Ming Li (2023-present), Brandon Manley (2023-present), Nick Baldonado (2022-present), Zardo Becker (2024-present).

Outline: helicity-dependent observables as RHIC and EIC at small x

- Sub-eikonal operators.
- DIS: Helicity PDFs and g_1 structure function at small x.
- Helicity evolution at small x.
- SIDIS: g_1^h structure function.
- Polarized p+p collisions: gluon production at mid-rapidity.
- OAM distributions at small x.
- Elastic dijet production in polarized e+p collisions.

Sub-Eikonal Operators

Dipole picture of DIS

$$W^{\mu\nu} = \frac{1}{4\pi M_p} \int d^4x\, e^{iq\cdot x}\, \langle P|j^\mu(x)\, j^\nu(0)|P\rangle$$

$$q^\mu = \left(\frac{Q^2}{2q^-}, q^-, 0_\perp\right)$$

Large q^- → large x^- separation

$$e^{iq\cdot x} = e^{i\frac{Q^2}{2q^-}x^- + iq^- x^+}$$

$$x^\pm = \frac{t \pm z}{\sqrt{2}}$$

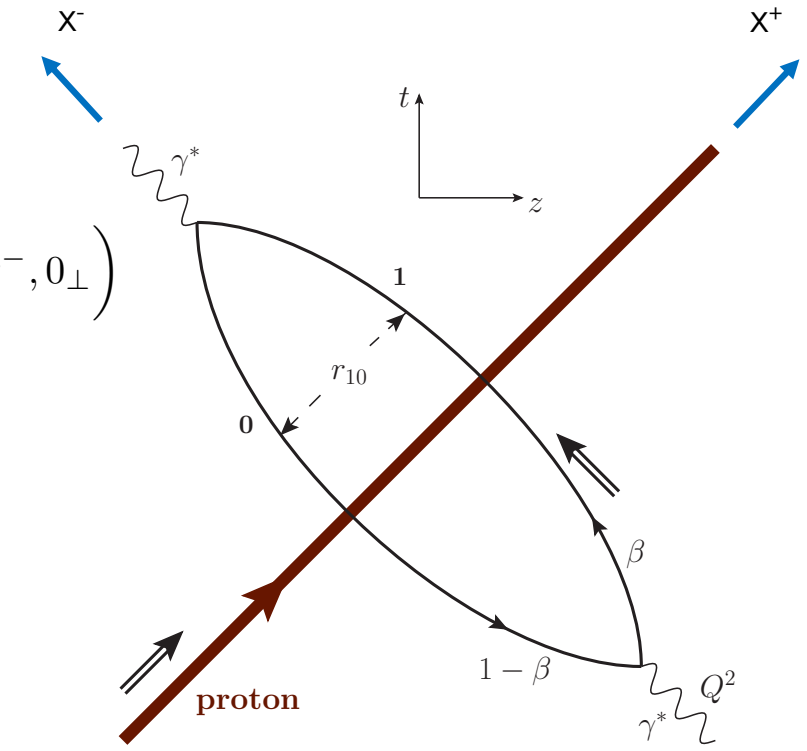

aka the "shock wave"

Polarized Dipole: non-eikonal small-x physics

- All flavor-singlet small-x helicity observables depend on "polarized dipole amplitudes":

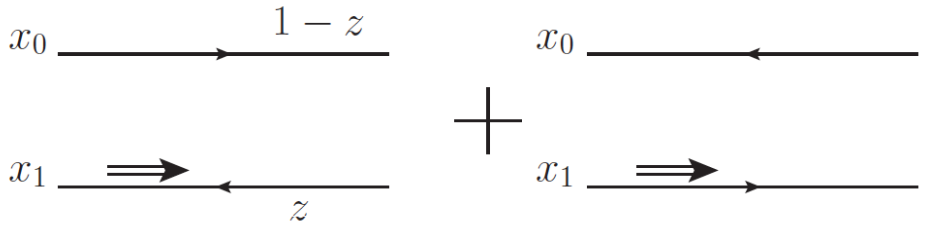

$$G_{10}(z) \equiv \frac{1}{2N_c}\,\mathrm{Re}\left\langle\!\!\left\langle \mathrm{T\,tr}\left[V_{\underline{0}} V_{\underline{1}}^{pol\,\dagger}\right] + \mathrm{T\,tr}\left[V_{\underline{1}}^{pol} V_{\underline{0}}^{\dagger}\right] \right\rangle\!\!\right\rangle(z)$$

unpolarized quark

polarized quark: eikonal propagation, non-eikonal spin-dependent interaction

$$V_{\underline{x}} = \mathcal{P}\exp\left[ig\int_{-\infty}^{\infty} dx^- A^+(0^+, x^-, \underline{x})\right]$$

- Double brackets denote an object with energy suppression scaled out:

$$\left\langle\!\!\left\langle \mathcal{O} \right\rangle\!\!\right\rangle(z) \equiv zs\left\langle \mathcal{O} \right\rangle(z)$$

Polarized fundamental "Wilson line"

- To complete the definition of the polarized dipole amplitude, we need to construct the definition of the polarized "Wilson line" V^{pol}, which is the leading helicity-dependent contribution for the quark scattering amplitude on a longitudinally-polarized target proton.

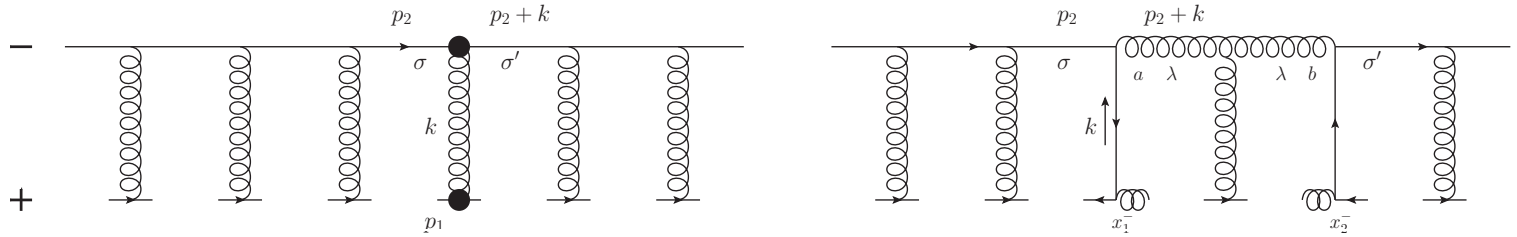

- At the leading order we can either exchange one non-eikonal *t*-channel gluon (with quark-gluon vertices denoted by blobs above) to transfer polarization between the projectile and the target, or two *t*-channel quarks, as shown above.
- We employ a blend of Brodsky & Lepage's LCPT and background field method-inspired operator treatment. We refer to the latter as the **light-cone operator treatment (LCOT)**.

Notation

- Fundamental light-cone Wilson line:

$$V_{\underline{x}}[b^-, a^-] = \mathrm{P} \exp\left\{ ig \int_{a^-}^{b^-} dx^- \, A^+(x^-, \underline{x}) \right\}$$

- Adjoint light-cone Wilson line:

$$U_{\underline{x}}[b^-, a^-] = \mathcal{P} \exp\left[ig \int_{a^-}^{b^-} dx^- \, \mathcal{A}^+(x^+ = 0, x^-, \underline{x}) \right]$$

- They sum multiple eikonal re-scatterings to all orders.

Eikonality

- One can classify various quantities (e.g.,TMDs) by their small-*x* asymptotics.
- Eikonal behavior corresponds to (up to ~α_S corrections in the power) $f(x, k_T^2) \sim \frac{1}{x}$
  Examples: unpolarized TMDs, Sivers function.
- Sub-eikonal behavior corresponds to $g(x, k_T^2) \sim \left(\frac{1}{x}\right)^0 = \text{const}$
  Example: helicity TMDs.
- Sub-sub-eikonal behavior is $h(x, k_T^2) \sim x$
  Examples: transversity, Boer-Mulder function.
- We've been calling the leading power of x "eikonality".

Sub-eikonal quark S-matrix in background gluon and quark fields

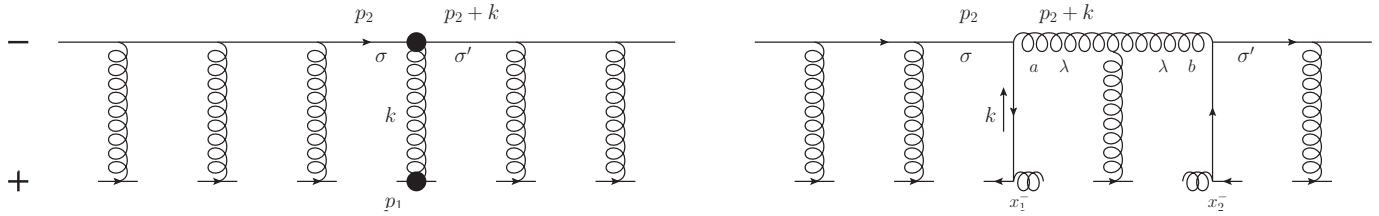

- The full sub-eikonal S-matrix for massless quarks is (Balitsky&Tarasov '15; KPS '17; YK, Sievert, '18; Chirilli '18; Altinoluk et al, '20; YK, Santiago '21)

$$V_{\underline{x},\underline{y};\sigma',\sigma} = V_{\underline{x}}\,\delta^2(\underline{x}-\underline{y})\,\delta_{\sigma,\sigma'}$$

"helicity independent" "helicity dependent"

$$-\vec{\mu}\cdot\vec{B} = -\mu_z\,B_z = \mu_z\,F^{12}$$

$$+\frac{i\,P^+}{s}\int_{-\infty}^{\infty} dz^-d^2z\;V_{\underline{x}}[\infty,z^-]\,\delta^2(\underline{x}-\underline{z})\left[-\delta_{\sigma,\sigma'}\overleftarrow{D}^i\;D^i+g\,\sigma\,\delta_{\sigma,\sigma'}\,F^{12}\right](z^-,\underline{z})\,V_{\underline{y}}[z^-,-\infty]\,\delta^2(\underline{y}-\underline{z})$$

$$-\frac{g^2P^+}{2s}\delta^2(\underline{x}-\underline{y})\int_{-\infty}^{\infty}dz_1^-\int_{z_1^-}^{\infty}dz_2^-\,V_{\underline{x}}[\infty,z_2^-]t^b\psi_\beta(z_2^-,\underline{x})U^{ba}_{\underline{x}}[z_2^-,z_1^-]\left[\delta_{\sigma,\sigma'}\gamma^+-\sigma\delta_{\sigma,\sigma'}\gamma^+\gamma^5\right]_{\alpha\beta}\bar{\psi}_\alpha(z_1^-,\underline{x})t^aV_{\underline{x}}[z_1^-,-\infty]$$

"helicity independent" "helicity dependent"

Longitudinal momentum transfer

In addition to the above, there is x+ dependence in the regular Wilson line, which is usually neglected in the eikonal approximation. If we expand in x+, we get a sub-eikonal correction

$$\int\limits_{-\infty}^{\infty} dx^+ \, e^{-i(p_f^- - p_i^-)\,x^+} \, V_{\underline{x}}(x^+) = \int\limits_{-\infty}^{\infty} dx^+ \, e^{-i(p_f^- - p_i^-)\,x^+} \, \left[V_{\underline{x}}(0^+) + x^+ \, \partial^- V_{\underline{x}}(0^+) + \ldots \right]$$

$$= 2\pi \, \delta(p_f^- - p_i^-) \, V_{\underline{x}}(0^+) - 2\pi \, i \left[\frac{\partial}{\partial p_f^-} \delta(p_f^- - p_i^-) \right] 2\sqrt{p_f^- \, p_i^-} \, V_{\underline{x}}^{\mathrm{G}[3]} + \ldots \, .$$

where we have introduced another "helicity-independent" sub-eikonal operator (Altinoluk et al, '20; c.f. Chirilli, '18)

$$V_{\underline{x}}^{\mathrm{G}[3]} = \frac{i \, g \, P^+}{s} \int\limits_{-\infty}^{\infty} dx^- V_{\underline{x}}[\infty, x^-] \, F^{+-}(x^-, \underline{x}) \, V_{\underline{x}}[x^-, -\infty].$$

This operator does not contribute to small-x helicity evolution at the leading order (DLA).

Helicity Distributions and g_1 Structure Function at Small x

Dipole Gluon Helicity TMD

- We start with the definition of the gluon dipole helicity TMD, corresponding to the Jaffe-Manohar PDF ΔG,

$$g_1^G(x,k_T^2) = \frac{-2i\,S_L}{x\,P^+}\int \frac{d\xi^-\,d^2\xi}{(2\pi)^3}\,e^{ixP^+\,\xi^- - i\underline{k}\cdot\underline{\xi}}\,\left\langle P,S_L|\epsilon_T^{ij}\,\mathrm{tr}\left[F^{+i}(0)\,\mathcal{U}^{[+]\dagger}[0,\xi]\,F^{+j}(\xi)\,\mathcal{U}^{[-]}[\xi,0]\right]|P,S_L\right\rangle_{\xi^+=0}$$

- Here $U^{[+]}$ and $U^{[-]}$ are future and past-pointing Wilson line staples (hence the name 'dipole' TMD, F. Dominguez et al '11 – looks like a dipole scattering on a proton):

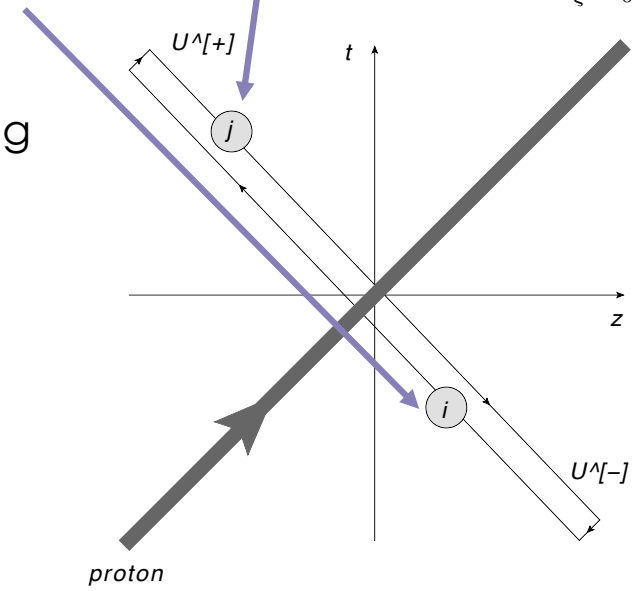

Gluon Helicity

- A calculation gives

$$\Delta G(x,Q^2) = \frac{2N_c}{\alpha_s \pi^2}\, G_2\left(\frac{1}{Q^2}, zs = \frac{Q^2}{x}\right)$$

$$g_{1L}^{G\,dip}(x,k_T^2) = \frac{N_c}{\alpha_s 2\pi^4}\int d^2x_{10}\, e^{-i\underline{k}\cdot\underline{x}_{10}}\, G_2\left(x_{10}^2, zs = \frac{Q^2}{x}\right)$$

- Here we defined a new dipole amplitude G_2 (cf. Hatta et al, 2016; KPS 2017)

$$\int d^2\left(\frac{x_1+x_0}{2}\right)\, G_{10}^i(zs) = (x_{10})_\perp^i\, G_1(x_{10}^2, zs) + \epsilon^{ij}\,(x_{10})_\perp^j\, G_2(x_{10}^2, zs)$$

$$G_{10}^j(zs) \equiv \frac{1}{2N_c}\left\langle\!\!\left\langle \mathrm{tr}\left[V_{\underline{0}}^\dagger\, V_{\underline{1}}^{j\,\mathrm{G[2]}} + \left(V_{\underline{1}}^{j\,\mathrm{G[2]}}\right)^\dagger V_{\underline{0}}\right]\right\rangle\!\!\right\rangle$$

$$V_{\underline{z}}^{i\,\mathrm{G[2]}} \equiv \frac{P^+}{2s}\int_{-\infty}^{\infty} dz^-\, V_{\underline{z}}[\infty, z^-]\left[D^i(z^-,\underline{z}) - \overleftarrow{D}^i(z^-,\underline{z})\right] V_{\underline{z}}[z^-,-\infty]$$

What is this D-D operator? Turns out it is related to the DD operator from before.

Quark Helicity PDF and TMD

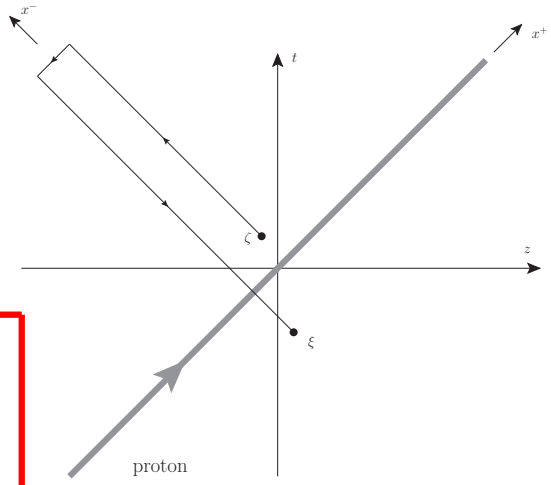

- The flavor-singlet quark helicity PDF and TMD are

$$\Delta\Sigma(x,Q^2) = \frac{N_f}{\alpha_s\,\pi^2}\,\widetilde{Q}\left(x_{10}^2 = \frac{1}{Q^2}, s = \frac{Q^2}{x}\right)$$

$$g_{1L}^S(x,k_T^2) = \frac{1}{4\pi^4\alpha_s}\int d^2x_{10}\,e^{-i\underline{k}\cdot\underline{x}_{10}}\;\widetilde{Q}(x_{10}^2, Q^2/x)$$

- We have defined another operator:

$$\widetilde{Q}_{12}(s) \equiv \left\langle\left\langle \frac{g^2}{16\sqrt{k^-\,p_2^-}}\int_{-\infty}^{\infty} dy^- \int_{-\infty}^{\infty} dz^- \left[\bar{\psi}(y^-,\underline{x}_2)\left(\frac{1}{2}\,\gamma^+\,\gamma^5\right) V_{\underline{2}}[y^-,\infty]\,V_{\underline{1}}[\infty,z^-]\,\psi(z^-,\underline{x}_1)\right.\right.\right.$$
$$\left.\left.\left. +\bar{\psi}(y^-,\underline{x}_2)\left(\frac{1}{2}\,\gamma^+\,\gamma^5\right) V_{\underline{2}}[y^-,-\infty]\,V_{\underline{1}}[-\infty,z^-]\,\psi(z^-,\underline{x}_1) + \text{c.c.}\right]\right\rangle\right\rangle(s).$$

g_1 structure function

- g_1 structure function is obtained similarly, using DIS in the dipole picture:

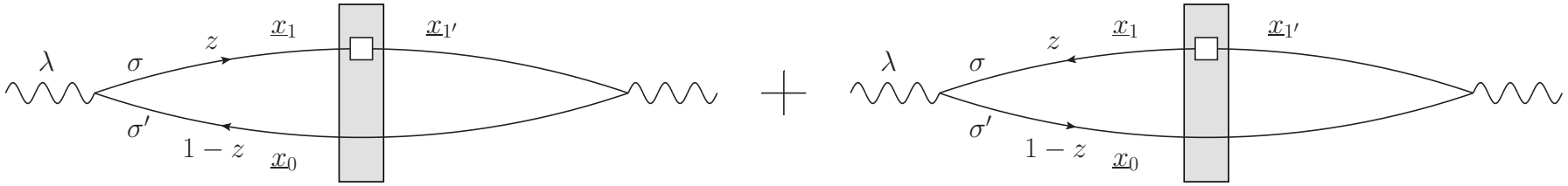

- One gets

$$g_1(x,Q^2) = -\sum_f \frac{N_c\, Z_f^2}{4\pi^3} \int\limits_{\Lambda^2/s}^{1} \frac{dz}{z} \int\limits_{\frac{1}{zs}}^{\min\left\{\frac{1}{zQ^2},\frac{1}{\Lambda^2}\right\}} \frac{dx_{10}^2}{x_{10}^2} \left[Q(x_{10}^2, zs) + 2\, G_2(x_{10}^2, zs)\right]$$

- G_2 was defined before. This is the gluon admixture to quark helicity distributions.
- The dipole amplitude Q is due to F^{12} & axial current.
- The contribution of G_2 comes from the DD operator in the quark S-matrix.

Amplitude Q

$$Q(x_{10}^2, zs) \equiv \int d^2 \left(\frac{x_0 + x_1}{2} \right) Q_{10}(zs)$$

- The amplitude Q is defined by

$$Q_{10}(zs) \equiv \frac{1}{2N_c} \,\mathrm{Re}\left\langle\!\!\left\langle \mathrm{T}\,\mathrm{tr}\left[V_{\underline{0}}\, V_{\underline{1}}^{\mathrm{pol}[1]\,\dagger}\right] + \mathrm{T}\,\mathrm{tr}\left[V_{\underline{1}}^{\mathrm{pol}[1]}\, V_{\underline{0}}^{\dagger}\right] \right\rangle\!\!\right\rangle$$

with $V_{\underline{x}}^{\mathrm{pol}[1]} = V_{\underline{x}}^{\mathrm{G}[1]} + V_{\underline{x}}^{\mathrm{q}[1]}$, where

$$V_{\underline{x}}^{\mathrm{G}[1]} = \frac{i\, g\, P^+}{s} \int_{-\infty}^{\infty} dx^- V_{\underline{x}}[\infty, x^-]\, F^{12}(x^-, \underline{x})\; V_{\underline{x}}[x^-, -\infty]$$

$$V_{\underline{x}}^{\mathrm{q}[1]} = \frac{g^2 P^+}{2\, s} \int_{-\infty}^{\infty} dx_1^- \int_{x_1^-}^{\infty} dx_2^- V_{\underline{x}}[\infty, x_2^-]\, t^b\, \psi_\beta(x_2^-, \underline{x})\, U_{\underline{x}}^{ba}[x_2^-, x_1^-]\; \left[\gamma^+\gamma^5\right]_{\alpha\beta}\; \bar{\psi}_\alpha(x_1^-, \underline{x})\, t^a\, V_{\underline{x}}[x_1^-, -\infty]$$

- U = adjoint light-cone Wilson line.

Helicity Evolution

Evolution for Polarized Quark Dipole

One can construct an evolution equation for the polarized dipole:

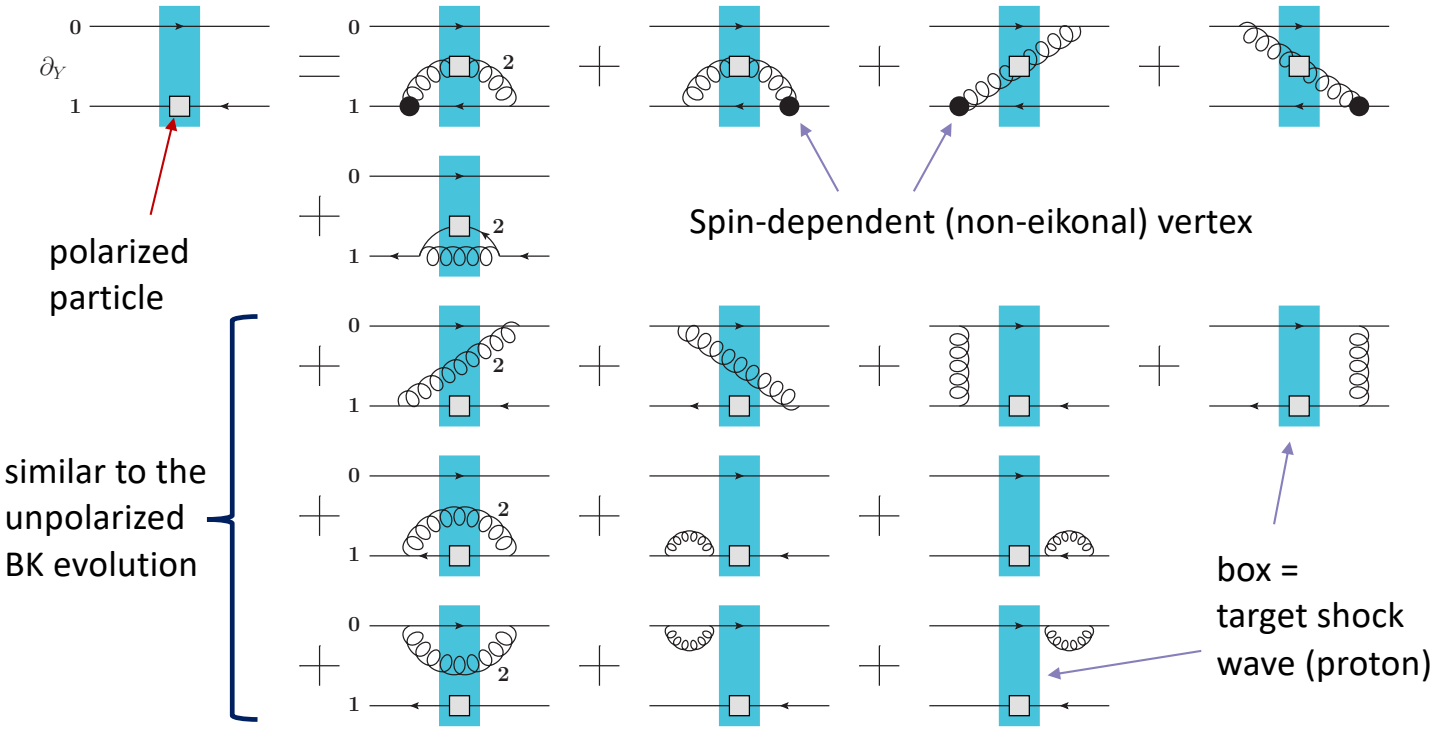

Large N_c

- At large-N_c the equations close (Q → G).
- Everything with 2 in the subscript (e.g., G_2 and Γ_2) is new (CTT+K) compared to the KPS ('15-'18) papers.

$$G(x_{10}^2, zs) = G^{(0)}(x_{10}^2, zs) + \frac{\alpha_s\, N_c}{2\pi} \int\limits_{\frac{1}{s x_{10}^2}}^{z} \frac{dz'}{z'} \int\limits_{\frac{1}{z's}}^{x_{10}^2} \frac{dx_{21}^2}{x_{21}^2} \Big[\Gamma(x_{10}^2, x_{21}^2, z's) + 3\, G(x_{21}^2, z's) + 2\, G_2(x_{21}^2, z's) + 2\, \Gamma_2(x_{10}^2, x_{21}^2, z's) \Big],$$

$$\Gamma(x_{10}^2, x_{21}^2, z's) = G^{(0)}(x_{10}^2, z's) + \frac{\alpha_s\, N_c}{2\pi} \int\limits_{\frac{1}{s x_{10}^2}}^{z'} \frac{dz''}{z''} \int\limits_{\frac{1}{z''s}}^{\min\left[x_{10}^2, x_{21}^2 \frac{z'}{z''}\right]} \frac{dx_{32}^2}{x_{32}^2} \Big[\Gamma(x_{10}^2, x_{32}^2, z''s) + 3\, G(x_{32}^2, z''s) + 2\, G_2(x_{32}^2, z''s) + 2\, \Gamma_2(x_{10}^2, x_{32}^2, z''s) \Big],$$

$$G_2(x_{10}^2, zs) = G_2^{(0)}(x_{10}^2, zs) + \frac{\alpha_s\, N_c}{\pi} \int\limits_{\frac{\Lambda^2}{s}}^{z} \frac{dz'}{z'} \int\limits_{\max\left[x_{10}^2, \frac{1}{z's}\right]}^{\min\left[\frac{z}{z'} x_{10}^2, \frac{1}{\Lambda^2}\right]} \frac{dx_{21}^2}{x_{21}^2} \left[G(x_{21}^2, z's) + 2\, G_2(x_{21}^2, z's) \right],$$

$$\Gamma_2(x_{10}^2, x_{21}^2, z's) = G_2^{(0)}(x_{10}^2, z's) + \frac{\alpha_s\, N_c}{\pi} \int\limits_{\frac{\Lambda^2}{s}}^{z' \frac{x_{21}^2}{x_{10}^2}} \frac{dz''}{z''} \int\limits_{\max\left[x_{10}^2, \frac{1}{z''s}\right]}^{\min\left[\frac{z'}{z''} x_{21}^2, \frac{1}{\Lambda^2}\right]} \frac{dx_{32}^2}{x_{32}^2} \left[G(x_{32}^2, z''s) + 2\, G_2(x_{32}^2, z''s) \right]$$

Initial Conditions

- The initial conditions are given by the Born-level graphs

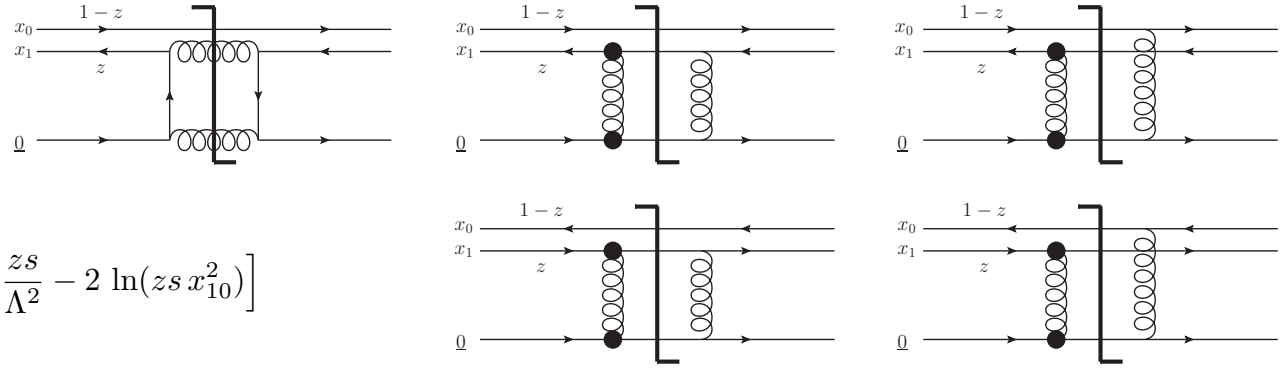

$$G^{(0)}(x_{10}^2, z) = \frac{\alpha_s^2 C_F}{N_c}\pi\left[C_F \ln\frac{zs}{\Lambda^2} - 2\,\ln(zs\,x_{10}^2)\right]$$

$$\Gamma^{(0)}(x_{10}^2, x_{21}^2, z) = G^{(0)}(x_{10}^2, z)$$

- Similar Born-level calculation is done for G_2 and Γ_2.

"Neighbor" dipole

- There is a new object in the evolution equation – **the neighbor dipole amplitude**.
- This is specific for the DLA evolution. Gluon emission may happen in one dipole, but, due to lifetime ordering, may 'know' about another dipole:

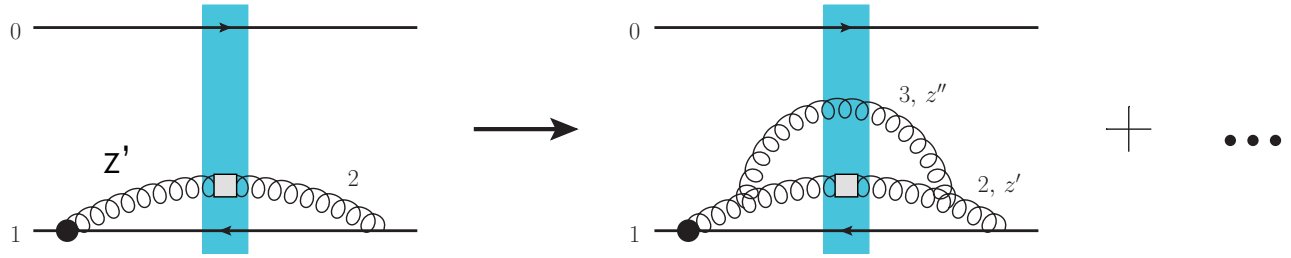

$$x_{21}^2\, z' \gg x_{32}^2\, z''$$

- We denote the evolution in the neighbor dipole 02 by $\Gamma_{02,\,21}(z')$

Helicity Evolution Ingredients

- Unlike the unpolarized evolution, in one step of helicity evolution we may emit a soft gluon or a soft quark (all in $A^- = 0$ LC gauge of the projectile):

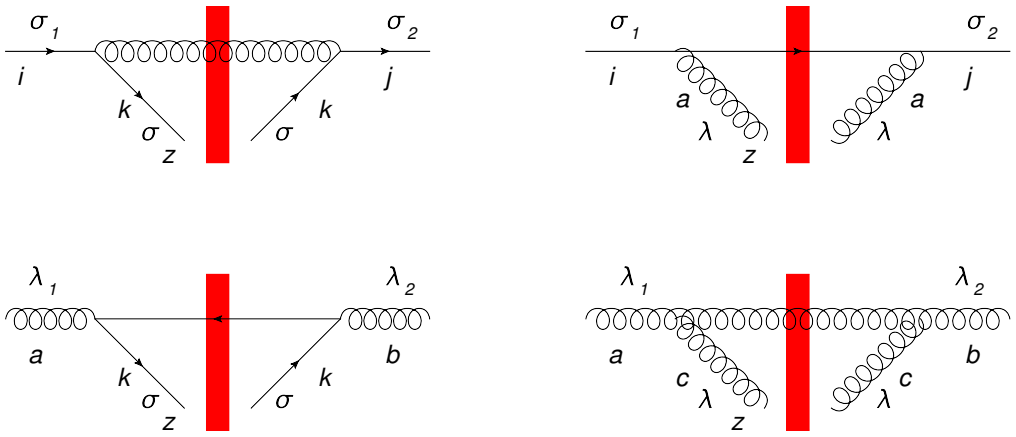

- When emitting gluons, one emission is eikonal, while another one is soft, but non-eikonal, as is needed to transfer polarization down the cascade/ladder.

Helicity Evolution: Ladders

- To get an idea of how the helicity evolution works let us try iterating the splitting kernels by considering ladder diagrams (circles denote non-eikonal gluon vertices):

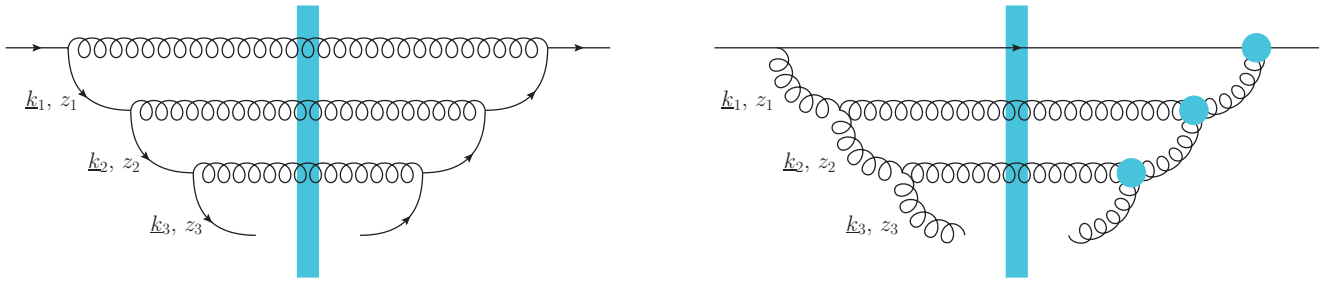

- To get the leading-energy asymptotics we need to order the longitudinal momentum fractions of the quarks and gluons (just like in the unpolarized evolution case) $1 \gg z_1 \gg z_2 \gg z_3 \gg \dots$

  obtaining a nested integral $\alpha_s^3 \int_{z_i}^{1} \frac{dz_1}{z_1} \int_{z_i}^{z_1} \frac{dz_2}{z_2} \int_{z_i}^{z_2} \frac{dz_3}{z_3}\, z_3 \otimes \frac{1}{z_3\, s} \sim \frac{1}{s}\, \alpha_s^3\, \ln^3 s$

Helicity Evolution: Ladders

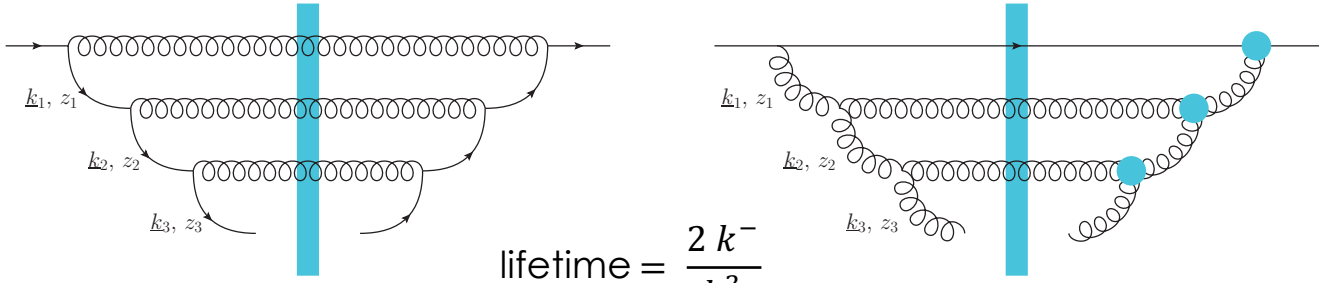

lifetime = $\dfrac{2\,k^-}{k_\perp^2}$

- However, these are not all the logs of energy one can get here. Transverse momentum (or distance) integrals have UV and IR divergences, which lead to logs of energy as well.
- If we order gluon/quark lifetimes as (Sudakov-β ordering) $\dfrac{2k_1^-}{\underline{k}_1^2} \gg \dfrac{2k_2^-}{\underline{k}_2^2} \gg \dfrac{2k_3^-}{\underline{k}_3^2} \gg \dots$ then ($z_i = k_i^-/p^-$). $\dfrac{\underline{k}_1^2}{z_1} \ll \dfrac{\underline{k}_2^2}{z_2} \ll \dfrac{\underline{k}_3^2}{z_3} \ll \dots$ and $z_1\,\underline{x}_1^2 \gg z_2\,\underline{x}_2^2 \gg z_3\,\underline{x}_3^2 \gg \dots$

  we would get integrals like $\displaystyle\int_{1/(z_n\,s)}^{x_{n-1,\perp}^2\,z_{n-1}/z_n} \dfrac{dx_{n,\perp}^2}{x_{n,\perp}^2}$ also generating logs of energy.

Helicity Evolution: Ladders

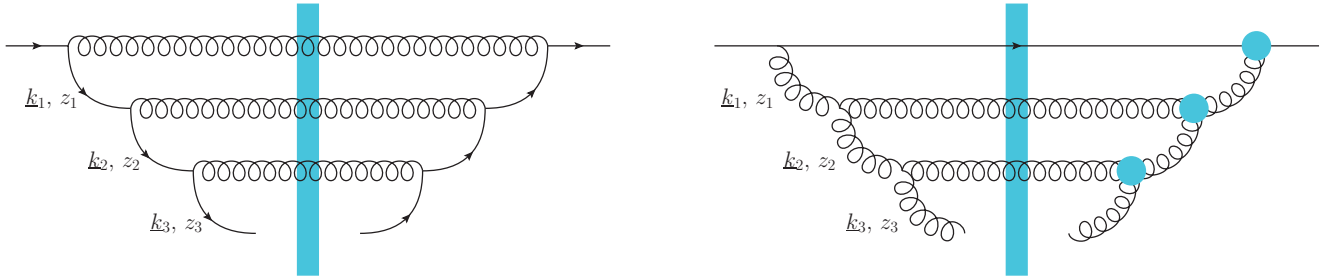

- To summarize, the above ladder diagrams are parametrically of the order

$$\frac{1}{s}\,\alpha_s^3\,\ln^6 s$$

- Note two features:
  - 1/s suppression due to non-eikonal exchange
  - two logs of energy per each power of the coupling!

Resummation Parameter

- For helicity evolution the leading resummation parameter is different from BFKL, BK or JIMWLK, which resum powers of leading logarithms (LLA)

$$\alpha_s \ln(1/x)$$

- Helicity evolution resummation parameter is double-logarithmic (DLA):

$$\alpha_s \ln^2 \frac{1}{x}$$

- The second logarithm of x arises due to transverse momentum (or transverse coordinate) integration being logarithmic both in the UV and IR.

- This was known before: Kirschner and Lipatov '83; Kirschner '84; Bartels, Ermolaev, Ryskin '95, '96; Griffiths and Ross '99; Itakura et al '03; Bartels and Lublinsky '03.

Large-N_c&N_f Evolution

- Helicity evolution equations also close in the large-N_c&N_f (Veneziano) limit.
- To derive those, need to add the transition diagrams (J. Borden, YK, M. Li, '24):

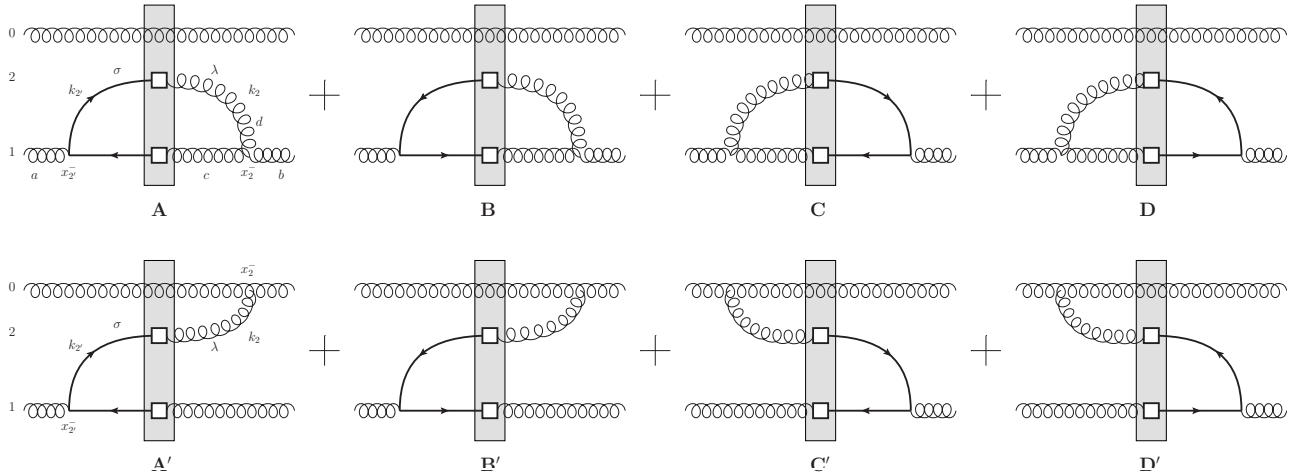

Evolution Equations

Initial version by YK, D. Pitonyak, M. Sievert '15-'18 (KPS), modifications with subscript 2 due to YK, F. Cougoulic, A. Tarasov, Y. Tawabutr '22.

Beyond large-N_c, one needs to add the quark-to-gluon and gluon-to-quark transitions (G. Chirilli, 2101.12744 [hep-ph]; J. Borden, YK, M. Li, 2406.11647 [hep-ph]):

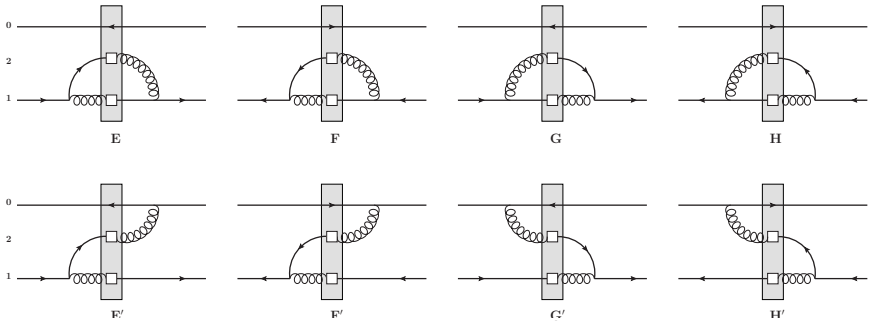

This results in the large-N_c&N_f evolution equations given here (transition terms are in blue). Agrees with DGLAP anomalous dimensions to 3 loops.

$$Q(x_{10}^2,zs) = Q^{(0)}(x_{10}^2,zs) + \frac{\alpha_s N_c}{2\pi}\int_{1/sx_{10}^2}^{z}\frac{dz'}{z'}\int_{1/z's}^{x_{10}^2}\frac{dx_{21}^2}{x_{21}^2}\Big[2\widetilde{G}(x_{21}^2,z's) + 2\widetilde{\Gamma}(x_{10}^2,x_{21}^2,z's) \tag{76a}$$
$$+ Q(x_{21}^2,z's) - \overline{\Gamma}(x_{10}^2,x_{21}^2,z's) + 2\Gamma_2(x_{10}^2,x_{21}^2,z's) + 2G_2(x_{21}^2,z's)\Big]$$
$$+ \frac{\alpha_s N_c}{4\pi}\int_{\Lambda^2/s}^{z}\frac{dz'}{z'}\int_{1/z's}^{\min\{x_{10}^2 z/z',1/\Lambda^2\}}\frac{dx_{21}^2}{x_{21}^2}\left[Q(x_{21}^2,z's) + 2G_2(x_{21}^2,z's)\right],$$

$$\overline{\Gamma}(x_{10}^2,x_{21}^2,z's) = Q^{(0)}(x_{10}^2,z's) + \frac{\alpha_s N_c}{2\pi}\int_{1/sx_{10}^2}^{z'}\frac{dz''}{z''}\int_{1/z''s}^{\min\{x_{10}^2,x_{21}^2 z'/z''\}}\frac{dx_{32}^2}{x_{32}^2}\Big[2\widetilde{G}(x_{32}^2,z''s) \tag{76b}$$
$$+ 2\widetilde{\Gamma}(x_{10}^2,x_{32}^2,z''s) + Q(x_{32}^2,z''s) - \overline{\Gamma}(x_{10}^2,x_{32}^2,z''s) + 2\Gamma_2(x_{10}^2,x_{32}^2,z''s) + 2G_2(x_{32}^2,z''s)\Big]$$
$$+ \frac{\alpha_s N_c}{4\pi}\int_{\Lambda^2/s}^{z'}\frac{dz''}{z''}\int_{1/z''s}^{\min\{x_{21}^2 z'/z'',1/\Lambda^2\}}\frac{dx_{32}^2}{x_{32}^2}\left[Q(x_{32}^2,z''s) + 2G_2(x_{32}^2,z''s)\right],$$

$$\widetilde{G}(x_{10}^2,zs) = \widetilde{G}^{(0)}(x_{10}^2,zs) + \frac{\alpha_s N_c}{2\pi}\int_{1/sx_{10}^2}^{z}\frac{dz'}{z'}\int_{1/z's}^{x_{10}^2}\frac{dx_{21}^2}{x_{21}^2}\Big[3\widetilde{G}(x_{21}^2,z's) + \widetilde{\Gamma}(x_{10}^2,x_{21}^2,z's) \tag{76c}$$
$$+ 2G_2(x_{21}^2,z's) + \left(2-\frac{N_f}{2N_c}\right)\Gamma_2(x_{10}^2,x_{21}^2,z's) - \frac{N_f}{4N_c}\overline{\Gamma}(x_{10}^2,x_{21}^2,z's) - \frac{N_f}{2N_c}\widetilde{Q}(x_{21}^2,z's)\Big]$$
$$- \frac{\alpha_s N_f}{8\pi}\int_{\Lambda^2/s}^{z}\frac{dz'}{z'}\int_{\max\{x_{10}^2,1/z's\}}^{\min\{x_{10}^2 z/z',1/\Lambda^2\}}\frac{dx_{21}^2}{x_{21}^2}\left[Q(x_{21}^2,z's) + 2G_2(x_{21}^2,z's)\right],$$

$$\widetilde{\Gamma}(x_{10}^2,x_{21}^2,z's) = \widetilde{G}^{(0)}(x_{10}^2,z's) + \frac{\alpha_s N_c}{2\pi}\int_{1/sx_{10}^2}^{z'}\frac{dz''}{z''}\int_{1/z''s}^{\min\{x_{10}^2,x_{21}^2 z'/z''\}}\frac{dx_{32}^2}{x_{32}^2}\Big[3\widetilde{G}(x_{32}^2,z''s) \tag{76d}$$
$$+ \widetilde{\Gamma}(x_{10}^2,x_{32}^2,z''s) + 2G_2(x_{32}^2,z''s) + \left(2-\frac{N_f}{2N_c}\right)\Gamma_2(x_{10}^2,x_{32}^2,z''s) - \frac{N_f}{4N_c}\overline{\Gamma}(x_{10}^2,x_{32}^2,z''s) - \frac{N_f}{2N_c}\widetilde{Q}(x_{32}^2,z''s)\Big]$$
$$- \frac{\alpha_s N_f}{8\pi}\int_{\Lambda^2/s}^{z'\frac{x_{21}^2}{x_{10}^2}}\frac{dz''}{z''}\int_{\max\{x_{10}^2,1/z''s\}}^{\min\{x_{21}^2 z'/z'',1/\Lambda^2\}}\frac{dx_{32}^2}{x_{32}^2}\left[Q(x_{32}^2,z''s) + 2G_2(x_{32}^2,z''s)\right],$$

$$G_2(x_{10}^2,zs) = G_2^{(0)}(x_{10}^2,zs) + \frac{\alpha_s N_c}{\pi}\int_{\frac{\Lambda^2}{s}}^{z}\frac{dz'}{z'}\int_{\max\left[x_{10}^2,\frac{1}{z's}\right]}^{\min\{\frac{z}{z'}x_{10}^2,1/\Lambda^2\}}\frac{dx_{21}^2}{x_{21}^2}\left[\widetilde{G}(x_{21}^2,z's) + 2G_2(x_{21}^2,z's)\right], \tag{76e}$$

$$\Gamma_2(x_{10}^2,x_{21}^2,z's) = G_2^{(0)}(x_{10}^2,z's) + \frac{\alpha_s N_c}{\pi}\int_{\frac{\Lambda^2}{s}}^{z'\frac{x_{21}^2}{x_{10}^2}}\frac{dz''}{z''}\int_{\max\left[x_{10}^2,\frac{1}{z''s}\right]}^{\min\{\frac{z'}{z''}x_{21}^2,1/\Lambda^2\}}\frac{dx_{32}^2}{x_{32}^2}\left[\widetilde{G}(x_{32}^2,z''s) + 2G_2(x_{32}^2,z''s)\right], \tag{76f}$$

$$\widetilde{Q}(x_{10}^2,zs) = \widetilde{Q}^{(0)}(x_{10}^2,zs) - \frac{\alpha_s N_c}{2\pi}\int_{\frac{\Lambda^2}{s}}^{z}\frac{dz'}{z'}\int_{\max\left[x_{10}^2,\frac{1}{z's}\right]}^{\min\{\frac{z}{z'}x_{10}^2,1/\Lambda^2\}}\frac{dx_{21}^2}{x_{21}^2}\left[Q(x_{21}^2,z's) + 2G_2(x_{21}^2,z's)\right]. \tag{76g}$$

Small-x Asymptotics

Solution of the Large-N_c Equations

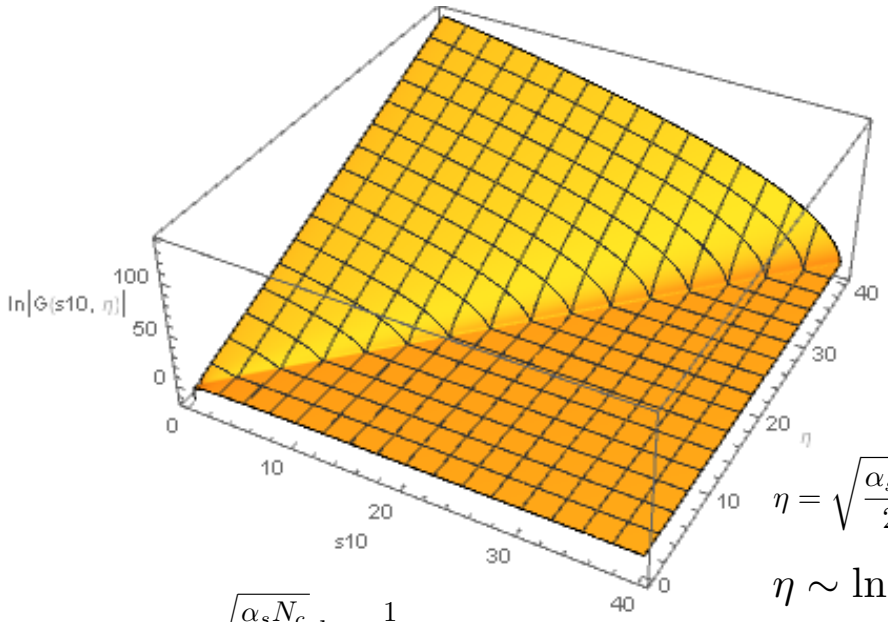

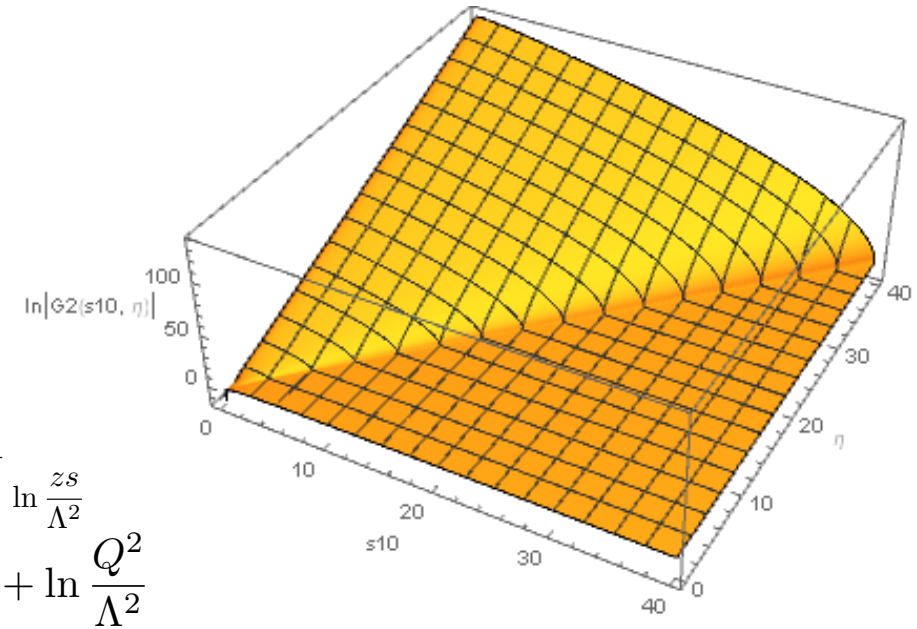

$$s_{10} = \sqrt{\frac{\alpha_s N_c}{2\pi}}\,\ln\frac{1}{x_{10}^2\,\Lambda^2}$$

$$s_{10} \sim \ln\frac{Q^2}{\Lambda^2}$$

$$\eta = \sqrt{\frac{\alpha_s N_c}{2\pi}}\,\ln\frac{zs}{\Lambda^2}$$

$$\eta \sim \ln\frac{1}{x} + \ln\frac{Q^2}{\Lambda^2}$$

The large-N_c equations for G and G_2 can be solved numerically (and, possibly, analytically).

Small-x Asymptotics

- Fitting the slope of the log plots of G and G_2 vs e we can read off the small-x intercept (the power of x):

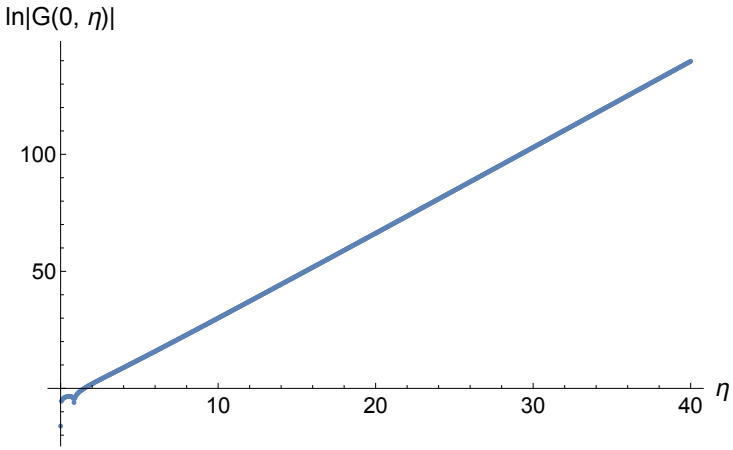

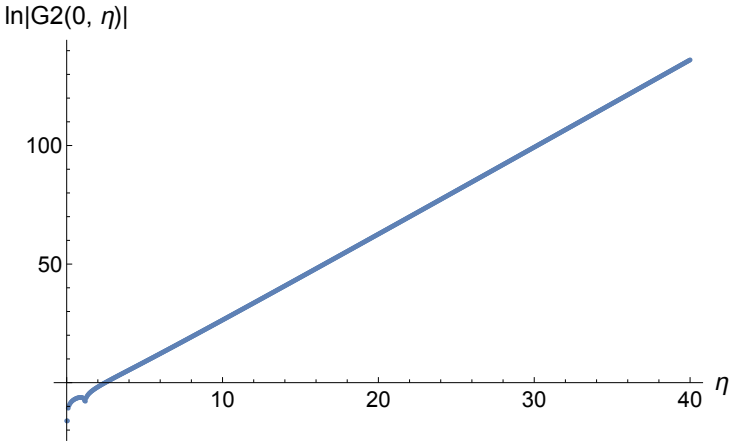

F. Cougoulic, YK, A. Tarasov, Y. Tawabutr, 2022

Small-x Asymptotics for Helicity Distributions

- The resulting small-x asymptotics for helicity PDFs and the g_1 structure function at large N_c is

$$\Delta\Sigma(x,Q^2) \sim \Delta G(x,Q^2) \sim g_1(x,Q^2) \sim \left(\frac{1}{x}\right)^{3.66\sqrt{\frac{\alpha_s\, N_c}{2\pi}}}$$

- This power (aka the intercept) is in complete agreement with the work by J. Bartels, B. Ermolaev, and M. Ryskin (BER, 1996) using infrared evolution equations (with the analytic intercept constructed by KPS in 2016):

$$\alpha_h = \sqrt{\frac{17+\sqrt{97}}{2}}\sqrt{\frac{\alpha_s\, N_c}{2\pi}} \approx 3.664\sqrt{\frac{\alpha_s\, N_c}{2\pi}}$$

- "Peace in the valley."
- **Right?**

Analytic Solution of the Large-N_c Equations

- We want to solve these equations:

$$G(x_{10}^2, zs) = G^{(0)}(x_{10}^2, zs) + \frac{\alpha_s\, N_c}{2\pi} \int\limits_{\frac{1}{s x_{10}^2}}^{z} \frac{dz'}{z'} \int\limits_{\frac{1}{z's}}^{x_{10}^2} \frac{dx_{21}^2}{x_{21}^2} \Big[\Gamma(x_{10}^2, x_{21}^2, z's) + 3\, G(x_{21}^2, z's) + 2\, G_2(x_{21}^2, z's) + 2\, \Gamma_2(x_{10}^2, x_{21}^2, z's) \Big],$$

$$\Gamma(x_{10}^2, x_{21}^2, z's) = G^{(0)}(x_{10}^2, z's) + \frac{\alpha_s\, N_c}{2\pi} \int\limits_{\frac{1}{s x_{10}^2}}^{z'} \frac{dz''}{z''} \int\limits_{\frac{1}{z''s}}^{\min\left[x_{10}^2, x_{21}^2 \frac{z'}{z''}\right]} \frac{dx_{32}^2}{x_{32}^2} \Big[\Gamma(x_{10}^2, x_{32}^2, z''s) + 3\, G(x_{32}^2, z''s) + 2\, G_2(x_{32}^2, z''s) + 2\, \Gamma_2(x_{10}^2, x_{32}^2, z''s) \Big],$$

$$G_2(x_{10}^2, zs) = G_2^{(0)}(x_{10}^2, zs) + \frac{\alpha_s\, N_c}{\pi} \int\limits_{\frac{\Lambda^2}{s}}^{z} \frac{dz'}{z'} \int\limits_{\max\left[x_{10}^2, \frac{1}{z's}\right]}^{\min\left[\frac{z}{z'} x_{10}^2, \frac{1}{\Lambda^2}\right]} \frac{dx_{21}^2}{x_{21}^2} \left[G(x_{21}^2, z's) + 2\, G_2(x_{21}^2, z's) \right],$$

$$\Gamma_2(x_{10}^2, x_{21}^2, z's) = G_2^{(0)}(x_{10}^2, z's) + \frac{\alpha_s\, N_c}{\pi} \int\limits_{\frac{\Lambda^2}{s}}^{z' \frac{x_{21}^2}{x_{10}^2}} \frac{dz''}{z''} \int\limits_{\max\left[x_{10}^2, \frac{1}{z''s}\right]}^{\min\left[\frac{z'}{z''} x_{21}^2, \frac{1}{\Lambda^2}\right]} \frac{dx_{32}^2}{x_{32}^2} \left[G(x_{32}^2, z''s) + 2\, G_2(x_{32}^2, z''s) \right]$$

Analytic Solution of the Large-N_c Equations

- The strategy is to use the double Laplace transform,

$$\bar{\alpha}_s \equiv \frac{\alpha_s\, N_c}{2\pi}$$

$$G_2(x_{10}^2, zs) = \int \frac{d\omega}{2\pi i} \int \frac{d\gamma}{2\pi i}\, e^{\omega \ln(zsx_{10}^2) + \gamma \ln\left(\frac{1}{x_{10}^2 \Lambda^2}\right)}\, G_{2\omega\gamma}$$

- One gets the expressions for all the other dipole amplitudes this way, for instance

$$G(x_{10}^2, zs) = \int \frac{d\omega}{2\pi i} \int \frac{d\gamma}{2\pi i}\, e^{\omega \ln(zsx_{10}^2) + \gamma \ln\left(\frac{1}{x_{10}^2 \Lambda^2}\right)} \left[\frac{\omega\gamma}{2\,\bar{\alpha}_s}\left(G_{2\omega\gamma} - G^{(0)}_{2\omega\gamma}\right) - 2\, G_{2\omega\gamma}\right]$$

- Neighbor amplitudes involve several different double Laplace transforms:

$$\Gamma_2(x_{10}^2, x_{21}^2, z's) = \int \frac{d\omega}{2\pi i} \int \frac{d\gamma}{2\pi i} \left[e^{\omega \ln(z'sx_{21}^2) + \gamma \ln\left(\frac{1}{x_{10}^2 \Lambda^2}\right)} \left(G_{2\omega\gamma} - G^{(0)}_{2\omega\gamma}\right) + e^{\omega \ln(z'sx_{10}^2) + \gamma \ln\left(\frac{1}{x_{10}^2 \Lambda^2}\right)} G^{(0)}_{2\omega\gamma}\right]$$

Analytic Solution of the Large-N_c Equations

- In the end, all the amplitudes in the double-Laplace space can be expressed in terms of the initial conditions/inhomogeneous terms, e.g.,

$$G_{2\omega\gamma} = G^{(0)}_{2\omega\gamma} + \frac{\bar{\alpha}_s}{\omega\left(\gamma-\gamma_\omega^-\right)\left(\gamma-\gamma_\omega^+\right)}\Bigg[2\left(\gamma-\delta_\omega^+\right)\left(G^{(0)}_{\delta_\omega^+\gamma}+2\,G^{(0)}_{2\,\delta_\omega^+\gamma}\right)-2\left(\gamma_\omega^+-\delta_\omega^+\right)\left(G^{(0)}_{\delta_\omega^+\gamma_\omega^+}+2\,G^{(0)}_{2\,\delta_\omega^+\gamma_\omega^+}\right)$$
$$+8\,\delta_\omega^-\left(G^{(0)}_{2\omega\gamma}-G^{(0)}_{2\omega\gamma_\omega^+}\right)\Bigg]$$

with

$$\delta_\omega^\pm = \frac{\omega}{2}\left[1\pm\sqrt{1-\frac{4\,\bar{\alpha}_s}{\omega^2}}\right] \qquad \gamma_\omega^\pm = \frac{\omega}{2}\left[1\pm\sqrt{1-\frac{16\,\bar{\alpha}_s}{\omega^2}\sqrt{1-\frac{4\,\bar{\alpha}_s}{\omega^2}}}\right]$$

- More details in J. Borden, YK, 2304.06161 [hep-ph].

Small-x Asymptotics for Helicity Distributions

- Let's take a closer look at the anomalous dimension:

$$\Delta G(x,Q^2) = \int \frac{d\omega}{2\pi i} \left(\frac{1}{x}\right)^{\omega} \left(\frac{Q^2}{\Lambda^2}\right)^{\Delta\gamma_{GG}(\omega)} \Delta G_\omega(\Lambda^2)$$

- In the pure-glue case, Bartels, Ermolaev and Ryskin's (BER) anomalous dimension can be found analytically. It reads (KPS '16)

$$\Delta\gamma_{GG}^{BER}(\omega) = \frac{1}{2}\left[\omega - \sqrt{\omega^2 - 16\,\bar{\alpha}_s \frac{1-\frac{3\,\bar{\alpha}_s}{\omega^2}}{1-\frac{\bar{\alpha}_s}{\omega^2}}}\right] \qquad \bar{\alpha}_s = \frac{\alpha_s\, N_c}{2\pi}$$

- Our evolution's anomalous dimension can be found analytically at large-N_c (J. Borden, YK, 2304.06161 [hep-ph]):

$$\Delta\gamma_{GG}^{us}(\omega) = \frac{1}{2}\left[\omega - \sqrt{\omega^2 - 16\,\bar{\alpha}_s \sqrt{1-\frac{4\,\bar{\alpha}_s}{\omega^2}}}\right]$$

A Tale of Two Anomalous Dimensions

- The two anomalous dimensions look similar enough but are not the same function.

$$\Delta\gamma_{GG}^{BER}(\omega) = \frac{1}{2}\left[\omega - \sqrt{\omega^2 - 16\,\bar{\alpha}_s \frac{1-\frac{3\,\bar{\alpha}_s}{\omega^2}}{1-\frac{\bar{\alpha}_s}{\omega^2}}}\right] \qquad \Delta\gamma_{GG}^{us}(\omega) = \frac{1}{2}\left[\omega - \sqrt{\omega^2 - 16\,\bar{\alpha}_s \sqrt{1-\frac{4\,\bar{\alpha}_s}{\omega^2}}}\right]$$

- Their expansions in α_S start out the same, then differ at four (!) loops (the first 3 terms agree with the existing finite-order calculations, the four-loop result is unknown):

$$\Delta\gamma_{GG}^{BER}(\omega) = \frac{4\,\bar{\alpha}_s}{\omega} + \frac{8\,\bar{\alpha}_s^2}{\omega^3} + \frac{56\,\bar{\alpha}_s^3}{\omega^5} + \frac{504\,\bar{\alpha}_s^4}{\omega^7} + \ldots$$

$$\Delta\gamma_{GG}^{us}(\omega) = \frac{4\,\bar{\alpha}_s}{\omega} + \frac{8\,\bar{\alpha}_s^2}{\omega^3} + \frac{56\,\bar{\alpha}_s^3}{\omega^5} + \frac{496\,\bar{\alpha}_s^4}{\omega^7} + \ldots$$

A Tale of Two Intercepts

$$\Delta G(x,Q^2) = \int \frac{d\omega}{2\pi i} \left(\frac{1}{x}\right)^{\omega} \left(\frac{Q^2}{\Lambda^2}\right)^{\Delta\gamma_{GG}(\omega)} \Delta G_\omega(\Lambda^2)$$

$$\Delta\gamma_{GG}^{BER}(\omega) = \frac{1}{2}\left[\omega - \sqrt{\omega^2 - 16\,\bar{\alpha}_s \frac{1-\frac{3\,\bar{\alpha}_s}{\omega^2}}{1-\frac{\bar{\alpha}_s}{\omega^2}}}\right] \qquad \Delta\gamma_{GG}^{us}(\omega) = \frac{1}{2}\left[\omega - \sqrt{\omega^2 - 16\,\bar{\alpha}_s\sqrt{1-\frac{4\,\bar{\alpha}_s}{\omega^2}}}\right]$$

- The intercept (largest power Re[ω]) is given by the right-most singularity (branch point) of the anomalous dimension.
- For BER this gives $\alpha_h = \sqrt{\frac{17+\sqrt{97}}{2}}\sqrt{\frac{\alpha_s\,N_c}{2\pi}} \approx 3.664\sqrt{\frac{\alpha_s\,N_c}{2\pi}}$
- For us $\alpha_h = \frac{4}{3^{1/3}}\sqrt{\mathrm{Re}\left[(-9+i\sqrt{111})^{1/3}\right]}\sqrt{\frac{\alpha_s\,N_c}{2\pi}} \approx 3.661\sqrt{\frac{\alpha_s\,N_c}{2\pi}}$

A Tale of Two Intercepts

$$\Delta\Sigma(x,Q^2)\Big|_{x\ll 1} \sim \Delta G(x,Q^2)\Big|_{x\ll 1} \sim \left(\frac{1}{x}\right)^{\alpha_h}$$

- The power α_h is known as the intercept.
- BER:

$$\alpha_h = \sqrt{\frac{17+\sqrt{97}}{2}}\sqrt{\frac{\alpha_s\, N_c}{2\pi}} \approx 3.664\sqrt{\frac{\alpha_s\, N_c}{2\pi}}$$

- Us:

$$\alpha_h = \frac{4}{3^{1/3}}\sqrt{\mathrm{Re}\left[(-9+i\sqrt{111})^{1/3}\right]}\sqrt{\frac{\alpha_s\, N_c}{2\pi}} \approx 3.661\sqrt{\frac{\alpha_s\, N_c}{2\pi}}$$

- Our numerical solution also gave the intercept of 3.660 or 3.661, but we believed we had larger error bars.
- We (still) disagree with BER. Albeit in the 3rd decimal point…

Analytic Solution of the Large-N_c&N_f Equations

- The same double inverse Laplace transform technique allowed us to solve the large-N_c&N_f evolution equations.
- See J. Borden, YK, 2508.00195 for details.
- We have the exact analytic solution (in terms of ω- and γ-integrals).
- We also have all 4 anomalous dimensions resumed to all orders in

$$\frac{\alpha_s}{\omega^2}$$

$$
\begin{aligned}
Q(x_{10}^2,zs) &= Q^{(0)}(x_{10}^2,zs) + \frac{\alpha_s N_c}{2\pi}\int_{1/sx_{10}^2}^{z}\frac{dz'}{z'}\int_{1/z's}^{x_{10}^2}\frac{dx_{21}^2}{x_{21}^2}\Big[2\widetilde{G}(x_{21}^2,z's) + 2\widetilde{\Gamma}(x_{10}^2,x_{21}^2,z's) \\
&\quad + Q(x_{21}^2,z's) - \overline{\Gamma}(x_{10}^2,x_{21}^2,z's) + 2\Gamma_2(x_{10}^2,x_{21}^2,z's) + 2G_2(x_{21}^2,z's)\Big] \\
&\quad + \frac{\alpha_s N_c}{4\pi}\int_{\Lambda^2/s}^{z}\frac{dz'}{z'}\int_{1/z's}^{\min\{x_{10}^2 z/z',1/\Lambda^2\}}\frac{dx_{21}^2}{x_{21}^2}\Big[Q(x_{21}^2,z's) + 2G_2(x_{21}^2,z's)\Big]\,, \qquad (76a)\\
\overline{\Gamma}(x_{10}^2,x_{21}^2,z's) &= Q^{(0)}(x_{10}^2,z's) + \frac{\alpha_s N_c}{2\pi}\int_{1/sx_{10}^2}^{z'}\frac{dz''}{z''}\int_{1/z''s}^{\min\{x_{10}^2,x_{21}^2 z'/z''\}}\frac{dx_{32}^2}{x_{32}^2}\Big[2\widetilde{G}(x_{32}^2,z''s) \\
&\quad + 2\widetilde{\Gamma}(x_{10}^2,x_{32}^2,z''s) + Q(x_{32}^2,z''s) - \overline{\Gamma}(x_{10}^2,x_{32}^2,z''s) + 2\Gamma_2(x_{10}^2,x_{32}^2,z''s) + 2G_2(x_{32}^2,z''s)\Big] \\
&\quad + \frac{\alpha_s N_c}{4\pi}\int_{\Lambda^2/s}^{z'}\frac{dz''}{z''}\int_{1/z''s}^{\min\{x_{21}^2 z'/z'',1/\Lambda^2\}}\frac{dx_{32}^2}{x_{32}^2}\Big[Q(x_{32}^2,z''s) + 2G_2(x_{32}^2,z''s)\Big]\,, \qquad (76b)\\
\widetilde{G}(x_{10}^2,zs) &= \widetilde{G}^{(0)}(x_{10}^2,zs) + \frac{\alpha_s N_c}{2\pi}\int_{1/sx_{10}^2}^{z}\frac{dz'}{z'}\int_{1/z's}^{x_{10}^2}\frac{dx_{21}^2}{x_{21}^2}\Big[3\widetilde{G}(x_{21}^2,z's) + \widetilde{\Gamma}(x_{10}^2,x_{21}^2,z's) \\
&\quad + 2G_2(x_{21}^2,z's) + \Big(2-\frac{N_f}{2N_c}\Big)\Gamma_2(x_{10}^2,x_{21}^2,z's) - \frac{N_f}{4N_c}\overline{\Gamma}(x_{10}^2,x_{21}^2,z's) - \frac{N_f}{2N_c}\widetilde{Q}(x_{21}^2,z's)\Big] \\
&\quad - \frac{\alpha_s N_f}{8\pi}\int_{\Lambda^2/s}^{z}\frac{dz'}{z'}\int_{\max\{x_{10}^2,1/z's\}}^{\min\{x_{10}^2 z/z',1/\Lambda^2\}}\frac{dx_{21}^2}{x_{21}^2}\Big[Q(x_{21}^2,z's) + 2G_2(x_{21}^2,z's)\Big]\,, \qquad (76c)\\
\widetilde{\Gamma}(x_{10}^2,x_{21}^2,z's) &= \widetilde{G}^{(0)}(x_{10}^2,z's) + \frac{\alpha_s N_c}{2\pi}\int_{1/sx_{10}^2}^{z'}\frac{dz''}{z''}\int_{1/z''s}^{\min\{x_{10}^2,x_{21}^2 z'/z''\}}\frac{dx_{32}^2}{x_{32}^2}\Big[3\widetilde{G}(x_{32}^2,z''s) \\
&\quad + \widetilde{\Gamma}(x_{10}^2,x_{32}^2,z''s) + 2G_2(x_{32}^2,z''s) + \Big(2-\frac{N_f}{2N_c}\Big)\Gamma_2(x_{10}^2,x_{32}^2,z''s) - \frac{N_f}{4N_c}\overline{\Gamma}(x_{10}^2,x_{32}^2,z''s) - \frac{N_f}{2N_c}\widetilde{Q}(x_{32}^2,z''s)\Big] \\
&\quad - \frac{\alpha_s N_f}{8\pi}\int_{\Lambda^2/s}^{z'x_{21}^2/x_{10}^2}\frac{dz''}{z''}\int_{\max\{x_{10}^2,1/z''s\}}^{\min\{x_{21}^2 z'/z'',1/\Lambda^2\}}\frac{dx_{32}^2}{x_{32}^2}\Big[Q(x_{32}^2,z''s) + 2G_2(x_{32}^2,z''s)\Big]\,, \qquad (76d)\\
G_2(x_{10}^2,zs) &= G_2^{(0)}(x_{10}^2,zs) + \frac{\alpha_s N_c}{\pi}\int_{\frac{\Lambda^2}{s}}^{z}\frac{dz'}{z'}\int_{\max\left[x_{10}^2,\frac{1}{z's}\right]}^{\min\{\frac{z}{z'}x_{10}^2,1/\Lambda^2\}}\frac{dx_{21}^2}{x_{21}^2}\Big[\widetilde{G}(x_{21}^2,z's) + 2G_2(x_{21}^2,z's)\Big]\,, \qquad (76e)\\
\Gamma_2(x_{10}^2,x_{21}^2,z's) &= G_2^{(0)}(x_{10}^2,z's) + \frac{\alpha_s N_c}{\pi}\int_{\frac{\Lambda^2}{s}}^{z'\frac{z}{z'}\frac{x_{21}^2}{x_{10}^2}}\frac{dz''}{z''}\int_{\max\left[x_{10}^2,\frac{1}{z''s}\right]}^{\min\{\frac{z'}{z''}x_{21}^2,1/\Lambda^2\}}\frac{dx_{32}^2}{x_{32}^2}\Big[\widetilde{G}(x_{32}^2,z''s) + 2G_2(x_{32}^2,z''s)\Big]\,, \qquad (76f)\\
\widetilde{Q}(x_{10}^2,zs) &= \widetilde{Q}^{(0)}(x_{10}^2,zs) - \frac{\alpha_s N_c}{2\pi}\int_{\frac{\Lambda^2}{s}}^{z}\frac{dz'}{z'}\int_{\max\left[x_{10}^2,\frac{1}{z's}\right]}^{\min\{\frac{z}{z'}x_{10}^2,1/\Lambda^2\}}\frac{dx_{21}^2}{x_{21}^2}\Big[Q(x_{21}^2,z's) + 2G_2(x_{21}^2,z's)\Big]. \qquad (76g)
\end{aligned}
$$

Small-x asymptotics of helicity PDFs at large-N_c&N_f

- Now, the eigenvalues of the matrix of anomalous dimensions are

$$\gamma_\omega^{-\pm} \equiv \frac{1}{2}\left[\omega - \sqrt{\omega^2 + s_1(\omega) \pm \sqrt{s_2(\omega)}}\right]$$

- To find the intercept, we need to find the right-most singularity of those eigenvalues in ω–plane:

J. Borden, YK, 2508.00195

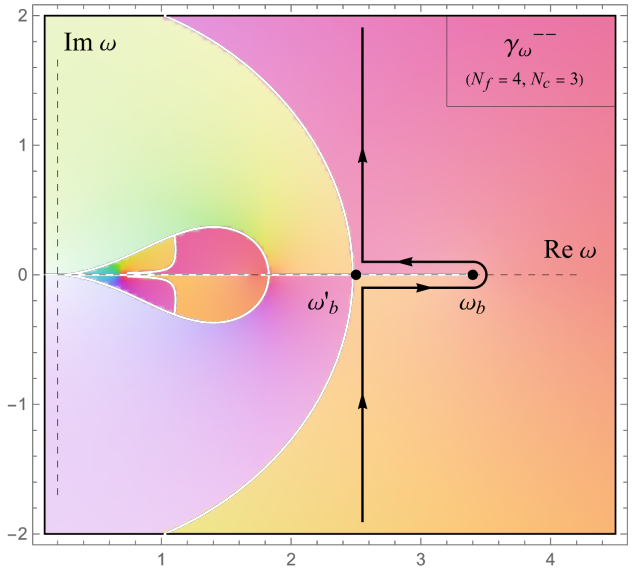

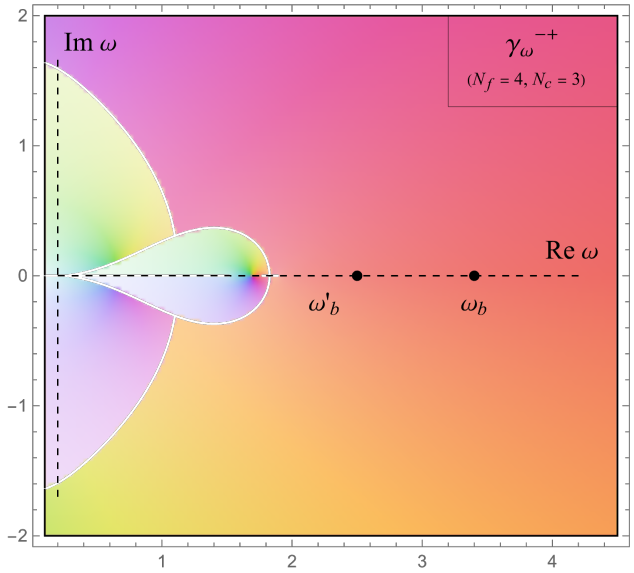

Small-x asymptotics of helicity PDFs at large-N_c&N_f

$$\Delta\Sigma(x,Q^2) \sim \Delta G(x,Q^2) \sim g_1(x,Q^2) \sim \left(\frac{1}{x}\right)^{\alpha_h} \quad \text{with} \quad \alpha_h \equiv \sqrt{\frac{\alpha_s\, N_c}{2\pi}}\,\omega_b$$

- To find the intercept, one has to solve the following algebraic equation:

$$\boxed{\omega_b^2 + s_1(\omega_b) - \sqrt{s_2(\omega_b)} = 0}$$

with

$$s_1(\omega) = -9 + \frac{2\,(8-3n)\,(\delta_\omega^{--}+\delta_\omega^{-+}) + 8\sqrt{4-2n}\,(\delta_\omega^{--}-\delta_\omega^{-+})}{\omega\,(2-n)},$$

$$s_2(\omega) = \frac{1}{(2-n)^2}\frac{1}{\omega^2}\Big\{\omega^2\,(2-n)^2\,(49-16n) - 64\,(2-n)\,(8-3n) + 8\omega\left(\delta_\omega^{--}+\delta_\omega^{-+}\right)\left(8+11n-7n^2\right)$$

$$+ 16\omega\left(\delta_\omega^{--}-\delta_\omega^{-+}\right)\sqrt{4-2n}\left(2+5n-2n^2\right) + 8n\delta_\omega^{--}\delta_\omega^{-+}\,(16-7n)\Big\}$$

where

$$\delta_\omega^{\pm\pm} \equiv \tfrac{1}{2}\left(\omega \pm \sqrt{\omega^2 \pm 4\sqrt{1-\tfrac{n}{2}}}\right) \qquad n = \frac{N_f}{N_c}$$

Small-x asymptotics of helicity PDFs at large-N_c&N_f

$$\Delta\Sigma(x,Q^2) \sim \Delta G(x,Q^2) \sim g_1(x,Q^2) \sim \left(\frac{1}{x}\right)^{\alpha_h} \quad \text{with} \quad \alpha_h \equiv \sqrt{\frac{\alpha_s\, N_c}{2\pi}}\,\omega_b$$

Solving the above algebraic equation numerically (and analytically for $N_f = 2\,N_c$), we get (for $N_c=3$)

N_f	$\omega_b^{(\mathrm{us})}$	$\omega_b^{(\mathrm{BER})}$	$\omega_b^{(\mathrm{BER})} - \omega_b^{(\mathrm{us})}$
2	3.54523	3.54816	0.00293
3	3.47910	3.48182	0.00272
4	3.40514	3.40757	0.00243
5	3.32036	3.32237	0.00201
6	$3.21930^{(*)}$	3.22062	0.00132
7	3.08946	3.08943	-0.00003
8	2.88228	2.87704	-0.00524

J. Borden, YK, 2508.00195

Small-x asymptotics of helicity PDFs at large-N_c&N_f

- Asymptotic expressions for hPDFs can be obtained by either integrating around the leading branch cut or by using the saddle point method. The latter gives

$$\Delta\Sigma(y,t) = \frac{e^{\omega_b y}}{y^{3/2}} \frac{N_f}{\alpha_s 8\pi^{5/2}}\, t\; e^{\frac{\omega_b}{2} t - \frac{\omega_b^2 C^{(1)}(\omega_b)}{16}\frac{t^2}{y}}\; \frac{\omega_b \sqrt{C^{(1)}(\omega_b)}}{s_1(\omega_b)+\omega_b^2} F_{\omega_b}^{(\Delta\Sigma)},$$

$$\Delta G(y,t) = \frac{e^{\omega_b y}}{y^{3/2}} \frac{N_c}{\alpha_s 4\pi^{5/2}}\, t\; e^{\frac{\omega_b}{2} t - \frac{\omega_b^2 C^{(1)}(\omega_b)}{16}\frac{t^2}{y}}\; \frac{\omega_b \sqrt{C^{(1)}(\omega_b)}}{s_1(\omega_b)+\omega_b^2} \left(\frac{s_1(\omega_b)+\omega_b^2}{\omega_b} - F_{\omega_b}^{(\Delta G)} \right)$$

with

$$y \equiv \sqrt{\frac{\alpha_s\, N_c}{2\pi}} \ln(1/x), \quad t \equiv \sqrt{\frac{\alpha_s\, N_c}{2\pi}} \ln(Q^2/\Lambda^2)$$

- Note the diffusion term, similar to that in the BFKL solution.

Asymptotic ratios of helicity PDFs

- One can also calculate the ratios of helicity PDFs at very small x , but still outside the saturation region (cf. Y. Hatta *et al*, 1612.02445, 1802.02716; R. Boussarie *et al*, 1904.02693):

N_f	ω_b	$(\Delta G/\Delta\Sigma)^{(\mathrm{asympt})}$
2	3.5452	-4.7871
3	3.4791	-3.0731
4	3.4051	-2.2075
5	3.3204	-1.6786
6	3.2193	-1.3143
7	3.0895	-1.0364
8	2.8823	-0.7872

J. Borden, YK, 2508.00195

- BER formalism gives $\Delta G(y,t) \approx -2.29\,\Delta\Sigma(y,t)$, R. Boussarie *et al*, 1904.02693 (N_f=4, N_c=3, not large N_c&N_f limit). We still disagree.

Polarized SIDIS
+ data analysis

D. Adamiak, N. Baldonado, YK, W. Melnitchouk, D. Pitonyak, N. Sato, M. Sievert, A. Tarasov, Y. Tawabutr, = JAMsmallx, 2308.07461 [hep-ph], 2503.21006 [hep-ph]

Polarized DIS and SIDIS data

- We can use the large-N_c&N_f version of the evolution to fit all the existing world polarized DIS and SIDIS data.
- Why not large-N_c? Have to distinguish a true quark dipole from the subset of the gluon one. Need to extract all helicity PDFs for light quark flavors, in addition to the gluon helicity PDF.
- Hence, the quark amplitudes Q_q come with the flavor index q.
- Drawback: many dipole amplitudes, hard to constrain all.
- LO intercept is large: had to include running coupling (not shown) into the evolution.

$$
\begin{aligned}
Q(x_{10}^2, zs) = Q^{(0)}(x_{10}^2, zs) &+ \frac{\alpha_s N_c}{2\pi} \int_{1/sx_{10}^2}^{z} \frac{dz'}{z'} \int_{1/z's}^{x_{10}^2} \frac{dx_{21}^2}{x_{21}^2} \Big[2\,\widetilde{G}(x_{21}^2, z's) + 2\,\widetilde{\Gamma}(x_{10}^2, x_{21}^2, z's) \\
&+ Q(x_{21}^2, z's) - \overline{\Gamma}(x_{10}^2, x_{21}^2, z's) + 2\,\Gamma_2(x_{10}^2, x_{21}^2, z's) + 2\,G_2(x_{21}^2, z's) \Big] \\
&+ \frac{\alpha_s N_c}{4\pi} \int_{\Lambda^2/s}^{z} \frac{dz'}{z'} \int_{1/z's}^{\min\{x_{10}^2 z/z', 1/\Lambda^2\}} \frac{dx_{21}^2}{x_{21}^2} \left[Q(x_{21}^2, z's) + 2\,G_2(x_{21}^2, z's) \right], \qquad (76a)
\end{aligned}
$$

$$
\begin{aligned}
\overline{\Gamma}(x_{10}^2, x_{21}^2, z's) = Q^{(0)}(x_{10}^2, z's) &+ \frac{\alpha_s N_c}{2\pi} \int_{1/sx_{10}^2}^{z'} \frac{dz''}{z''} \int_{1/z''s}^{\min\{x_{10}^2, x_{21}^2 z'/z''\}} \frac{dx_{32}^2}{x_{32}^2} \Big[2\,\widetilde{G}(x_{32}^2, z''s) \\
&+ 2\,\widetilde{\Gamma}(x_{10}^2, x_{32}^2, z''s) + Q(x_{32}^2, z''s) - \overline{\Gamma}(x_{10}^2, x_{32}^2, z''s) + 2\,\Gamma_2(x_{10}^2, x_{32}^2, z''s) + 2\,G_2(x_{32}^2, z''s) \Big] \\
&+ \frac{\alpha_s N_c}{4\pi} \int_{\Lambda^2/s}^{z'} \frac{dz''}{z''} \int_{1/z''s}^{\min\{x_{21}^2 z'/z'', 1/\Lambda^2\}} \frac{dx_{32}^2}{x_{32}^2} \left[Q(x_{32}^2, z''s) + 2\,G_2(x_{32}^2, z''s) \right], \qquad (76b)
\end{aligned}
$$

$$
\begin{aligned}
\widetilde{G}(x_{10}^2, zs) = \widetilde{G}^{(0)}(x_{10}^2, zs) &+ \frac{\alpha_s N_c}{2\pi} \int_{1/sx_{10}^2}^{z} \frac{dz'}{z'} \int_{1/z's}^{x_{10}^2} \frac{dx_{21}^2}{x_{21}^2} \Big[3\,\widetilde{G}(x_{21}^2, z's) + \widetilde{\Gamma}(x_{10}^2, x_{21}^2, z's) \\
&+ 2\,G_2(x_{21}^2, z's) + \left(2 - \frac{N_f}{2N_c} \right) \Gamma_2(x_{10}^2, x_{21}^2, z's) - \frac{N_f}{4N_c}\,\overline{\Gamma}(x_{10}^2, x_{21}^2, z's) - \frac{N_f}{2N_c}\,\widetilde{Q}(x_{21}^2, z's) \Big] \\
&- \frac{\alpha_s N_f}{8\pi} \int_{\Lambda^2/s}^{z} \frac{dz'}{z'} \int_{\max\{x_{10}^2, 1/z's\}}^{\min\{x_{10}^2 z/z', 1/\Lambda^2\}} \frac{dx_{21}^2}{x_{21}^2} \left[Q(x_{21}^2, z's) + 2\,G_2(x_{21}^2, z's) \right], \qquad (76c)
\end{aligned}
$$

$$
\begin{aligned}
\widetilde{\Gamma}(x_{10}^2, x_{21}^2, z's) = \widetilde{G}^{(0)}(x_{10}^2, z's) &+ \frac{\alpha_s N_c}{2\pi} \int_{1/sx_{10}^2}^{z'} \frac{dz''}{z''} \int_{1/z''s}^{\min\{x_{10}^2, x_{21}^2 z'/z''\}} \frac{dx_{32}^2}{x_{32}^2} \Big[3\,\widetilde{G}(x_{32}^2, z''s) \\
&+ \widetilde{\Gamma}(x_{10}^2, x_{32}^2, z''s) + 2\,G_2(x_{32}^2, z''s) + \left(2 - \frac{N_f}{2N_c} \right) \Gamma_2(x_{10}^2, x_{32}^2, z''s) - \frac{N_f}{4N_c}\,\overline{\Gamma}(x_{10}^2, x_{32}^2, z''s) - \frac{N_f}{2N_c}\,\widetilde{Q}(x_{32}^2, z''s) \Big] \\
&- \frac{\alpha_s N_f}{8\pi} \int_{\Lambda^2/s}^{z'x_{21}^2/x_{10}^2} \frac{dz''}{z''} \int_{\max\{x_{10}^2, 1/z''s\}}^{\min\{x_{21}^2 z'/z'', 1/\Lambda^2\}} \frac{dx_{32}^2}{x_{32}^2} \left[Q(x_{32}^2, z''s) + 2\,G_2(x_{32}^2, z''s) \right], \qquad (76d)
\end{aligned}
$$

$$
G_2(x_{10}^2, zs) = G_2^{(0)}(x_{10}^2, zs) + \frac{\alpha_s N_c}{\pi} \int_{\frac{\Lambda^2}{s}}^{z} \frac{dz'}{z'} \int_{\max\left[x_{10}^2, \frac{1}{z's}\right]}^{\min\{\frac{z}{z'} x_{10}^2, 1/\Lambda^2\}} \frac{dx_{21}^2}{x_{21}^2} \left[\widetilde{G}(x_{21}^2, z's) + 2\,G_2(x_{21}^2, z's) \right], \qquad (76e)
$$

$$
\Gamma_2(x_{10}^2, x_{21}^2, z's) = G_2^{(0)}(x_{10}^2, z's) + \frac{\alpha_s N_c}{\pi} \int_{\frac{\Lambda^2}{s}}^{z' \frac{x_{21}^2}{x_{10}^2}} \frac{dz''}{z''} \int_{\max\left[x_{10}^2, \frac{1}{z''s}\right]}^{\min\{\frac{z'}{z''} x_{21}^2, 1/\Lambda^2\}} \frac{dx_{32}^2}{x_{32}^2} \left[\widetilde{G}(x_{32}^2, z''s) + 2\,G_2(x_{32}^2, z''s) \right], \qquad (76f)
$$

$$
\widetilde{Q}(x_{10}^2, zs) = \widetilde{Q}^{(0)}(x_{10}^2, zs) - \frac{\alpha_s N_c}{2\pi} \int_{\frac{\Lambda^2}{s}}^{z} \frac{dz'}{z'} \int_{\max\left[x_{10}^2, \frac{1}{z's}\right]}^{\min\{\frac{z}{z'} x_{10}^2, 1/\Lambda^2\}} \frac{dx_{21}^2}{x_{21}^2} \left[Q(x_{21}^2, z's) + 2\,G_2(x_{21}^2, z's) \right]. \qquad (76g)
$$

Polarized SIDIS at small x

Consider (anti-)quark production in the current fragmentation region in the polarized e+p scattering at small x.

The process is similar to the g_1 structure function calculation.

A straightforward calculation yields the SIDIS structure function (D_1 = fragmentation function)

$$g_1^h(x,z,Q^2) \approx \frac{1}{2}\sum_{q,\bar{q}} e_q^2\,\Delta q(x,Q^2)\,D_1^{h/q}(z,Q^2)$$

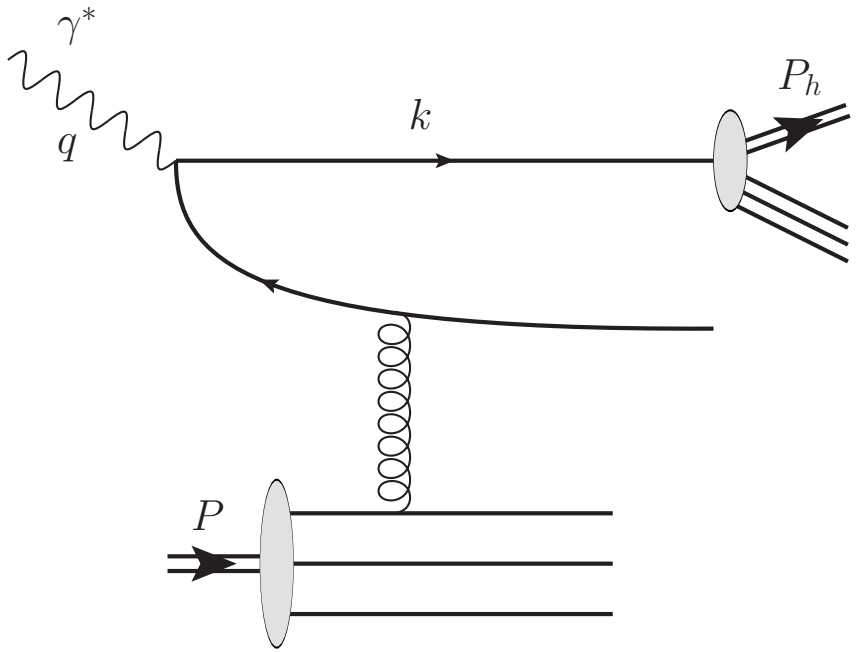

JAMsmallx: **Adamiak**, Baldonado, YK, Melnitchouk, Pitonyak, Sato, Sievert, Tarasov, Tawabutr, 2308.07461 [hep-ph]

The analysis

$$5 \times 10^{-3} < x < 0.1 \equiv x_0$$

$$\chi^2/N_{pts} = 1.03$$

$$1.69\ \mathrm{GeV}^2 < Q^2 < 10.4\ \mathrm{GeV}^2$$

Initial conditions: $Q^{(0)}(x_{10}^2, zs) \sim G_2^{(0)}(x_{10}^2, zs) \sim a\ \ln \frac{zs}{\Lambda^2} + b\ \ln \frac{1}{x_{10}^2 \Lambda^2} + c$

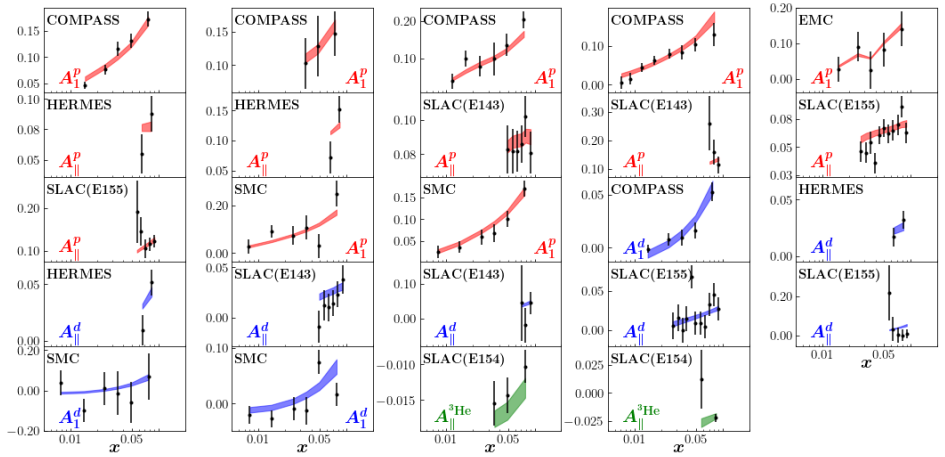

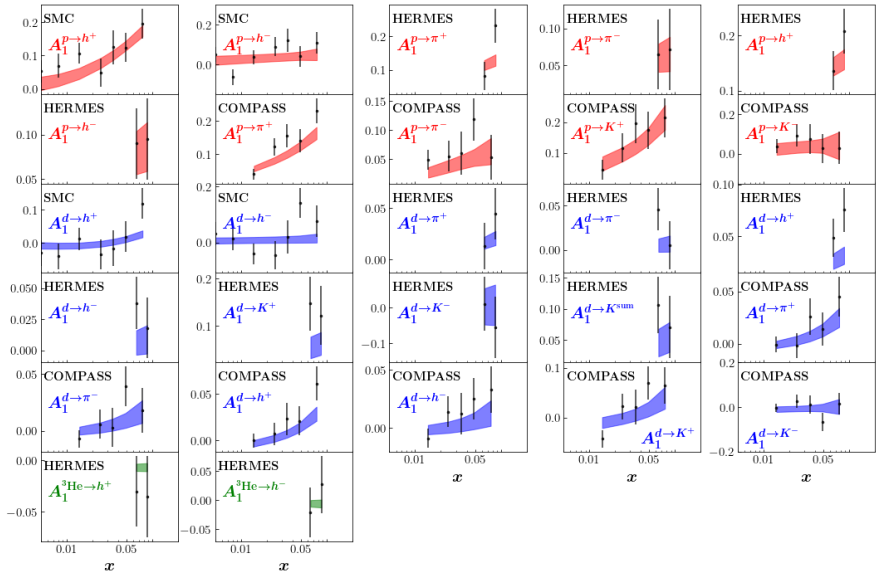

$$A_{\parallel} = \frac{\sigma^{\downarrow\Uparrow} - \sigma^{\uparrow\Uparrow}}{\sigma^{\downarrow\Uparrow} + \sigma^{\uparrow\Uparrow}}$$

$$A_1 \approx \frac{g_1}{F_1}$$

$$A_{\parallel} \approx D\, A_1$$

Double-spin asymmetries for p, d, and ^{3}He

D= kinematic factor (known)
Running-coupling large-N_c&N_f evolution, 226 polarized DIS and SIDIS data points.

Proton g_1 structure function

JAM-smallx

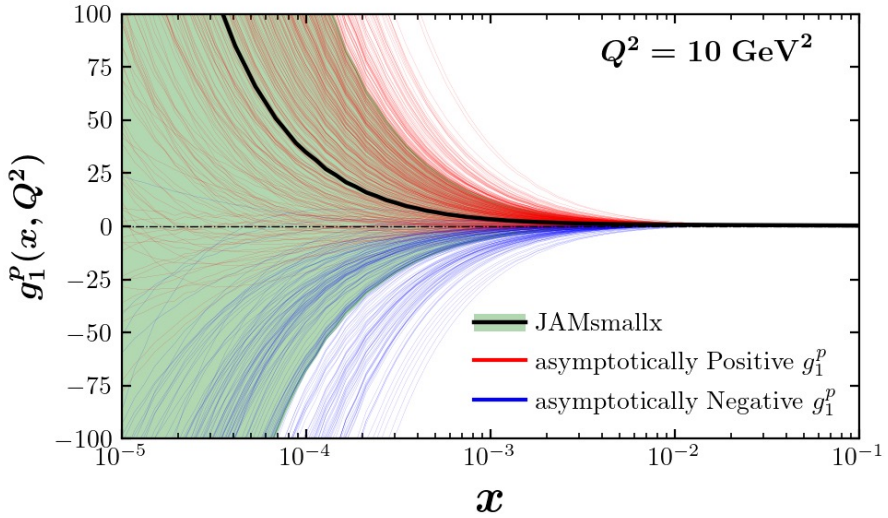

g_1^p extracted from the existing data

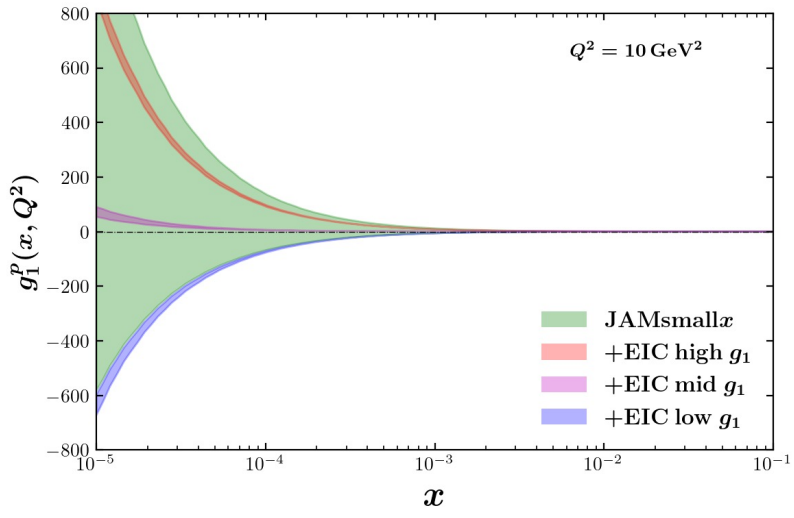

EIC impact

- JAM is based on a Bayesian Monte-Carlo: it uses replicas.
- Due to the lack of constraints, the spread is large.
- On the right, extraction using EIC pseudo-data (3 thin bands = 3 possible EIC data sets).

Helicity PDFs:

JAM-smallx

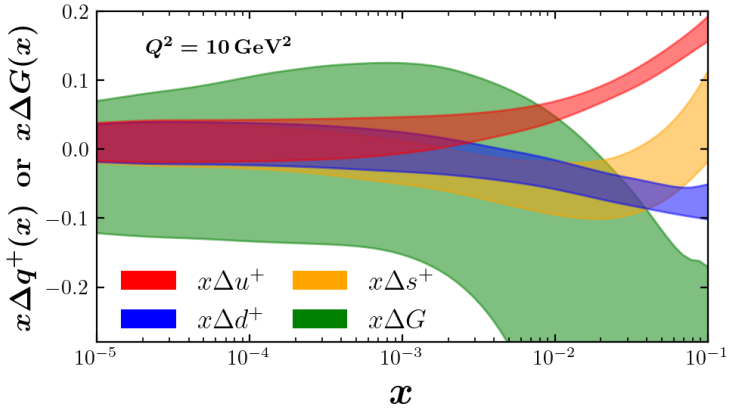

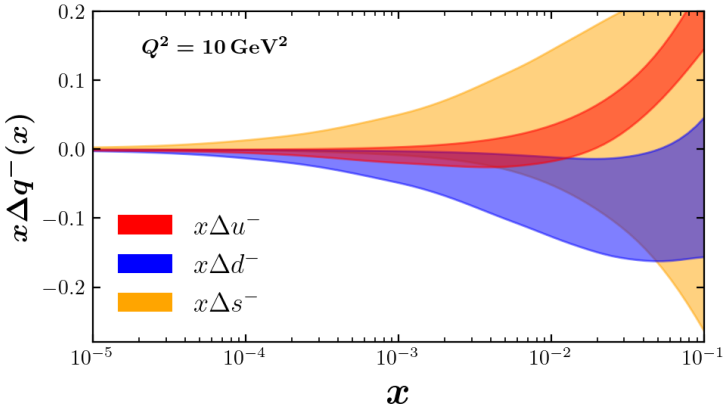

$$\Delta q^+ = \Delta q + \Delta\bar{q} \qquad \Delta q^- = \Delta q - \Delta\bar{q}$$

Uncertainties at small x seem to be driven by our inability to constrain the dipole amplitude G_2 and Gtilde using the current data.

JAMsmallx: Adamiak, Baldonado, YK, Melnitchouk, Pitonyak, Sato, Sievert, Tarasov, Tawabutr 2023

How much spin is there at small x?

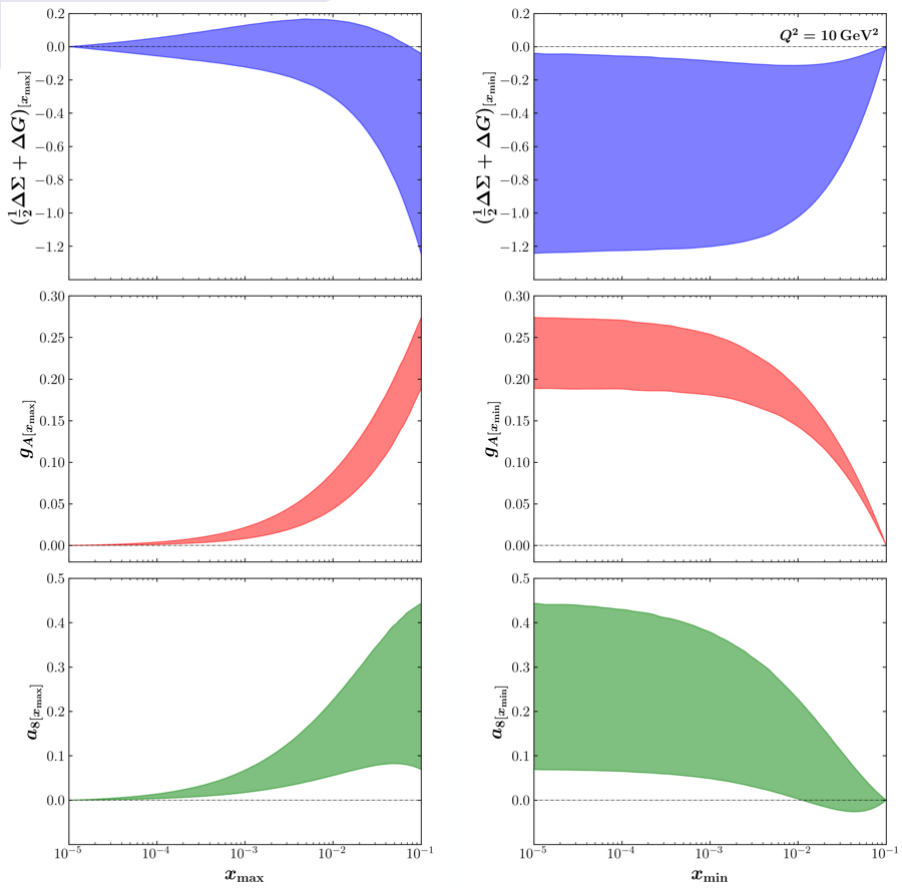

$$\left(\frac{1}{2}\Delta\Sigma + \Delta G\right)_{[x_{\min}]}(Q^2) \equiv \int_{x_{\min}}^{x_0} dx \left(\frac{1}{2}\Delta\Sigma + \Delta G\right)(x, Q^2),$$

$$g_{A[x_{\min}]}(Q^2) \equiv \int_{x_{\min}}^{x_0} dx \left[\Delta u^+(x, Q^2) - \Delta d^+(x, Q^2)\right],$$

$$a_{8[x_{\min}]}(Q^2) \equiv \int_{x_{\min}}^{x_0} dx \left[\Delta u^+(x, Q^2) + \Delta d^+(x, Q^2) - 2\,\Delta s^+(x, Q^2)\right]$$

$$\left(\frac{1}{2}\Delta\Sigma + \Delta G\right)_{[x_{\max}]}(Q^2) \equiv \int_{10^{-5}}^{x_{\max}} dx \left(\frac{1}{2}\Delta\Sigma + \Delta G\right)(x, Q^2),$$

$$g_{A[x_{\max}]}(Q^2) \equiv \int_{10^{-5}}^{x_{\max}} dx \left[\Delta u^+(x, Q^2) - \Delta d^+(x, Q^2)\right],$$

$$a_{8[x_{\max}]}(Q^2) \equiv \int_{10^{-5}}^{x_{\max}} dx \left[\Delta u^+(x, Q^2) + \Delta d^+(x, Q^2) - 2\,\Delta s^+(x, Q^2)\right]$$

$$\int_{10^{-5}}^{0.1} \mathrm{d}x \left(\frac{1}{2}\Delta\Sigma + \Delta G\right)(x) = -0.64 \pm 0.60$$

Negative net spin at small x!

Potentially a lot of spin at small x. However, the uncertainties are large. Need a way to constrain the initial conditions. To do so, we will include the polarized p+p data from RHIC.

Particle production in polarized p+p collisions

YK, M. Li, 2403.06959 [hep-ph]

Gluon production at mid-rapidity

- We want to calculate gluon production cross section in polarized p+p collisions at mid-rapidity, where the gluon is small-x in both proton's wave functions.

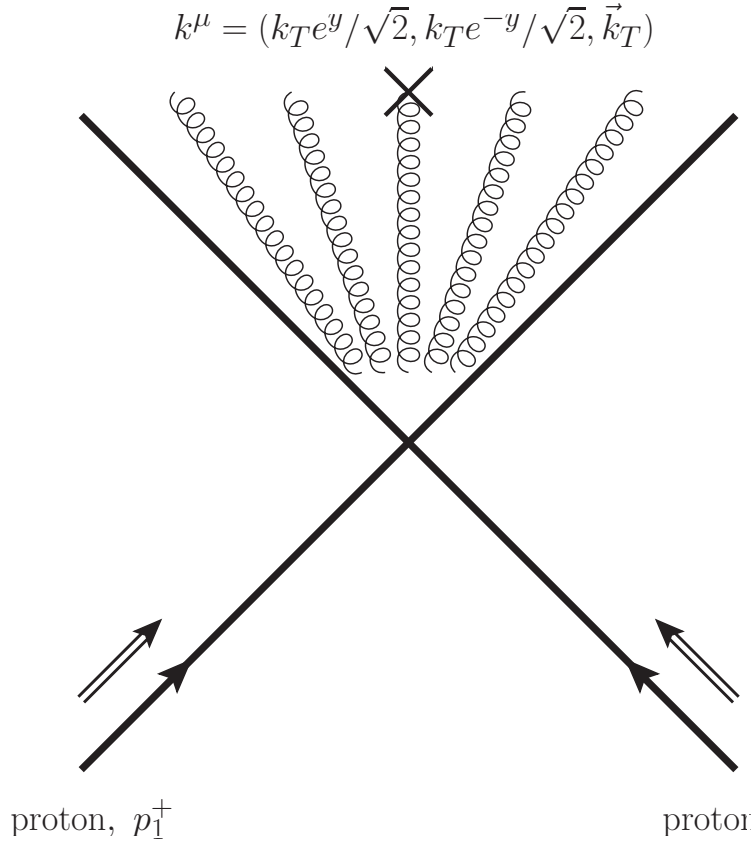

Gluon production in polarized p+p collisions

Working in the shock wave picture, we first need to sum up the following diagrams (emission inside shock wave is suppressed by a log):

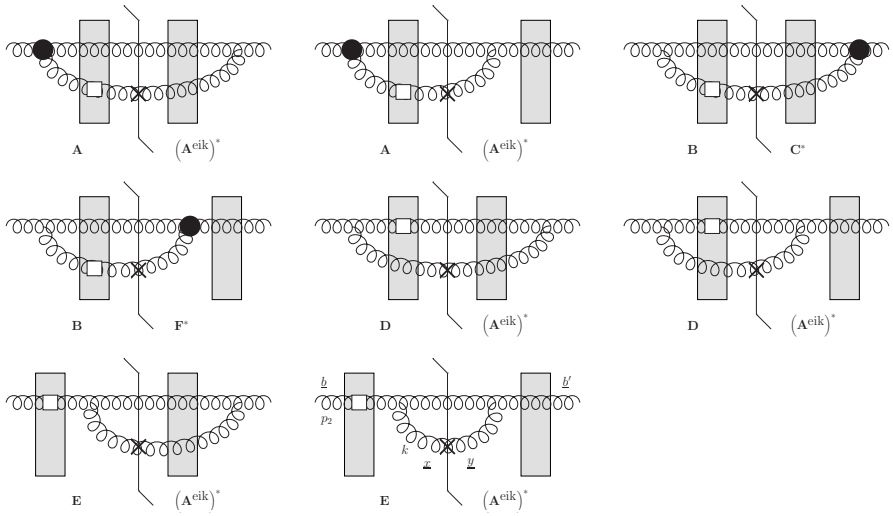

The result is shown below, and is cross-checked against the existing lowest-order calculations.

$$\frac{d\sigma(\lambda)}{d^2k_T\,dy} = \lambda\,\frac{\alpha_s}{\pi^4}\,\frac{1}{s}\,N_c\int d^2x\,d^2y\,d^2b\,e^{-i\underline{k}\cdot(\underline{x}-\underline{y})}\left\{\frac{\underline{x}-\underline{b}}{|\underline{x}-\underline{b}|^2}\cdot\frac{\underline{y}-\underline{b}}{|\underline{y}-\underline{b}|^2}\left[G^{\rm adj}_{\underline{x},\underline{y}}(2k^-p_1^+) - G^{\rm adj}_{\underline{x},\underline{b}}(2k^-p_1^+)\right.\right.$$
$$\left.\left. -\frac{1}{4}\left(G^{\rm adj}_{\underline{b},\underline{y}}(2k^-p_1^+) + G^{\rm adj}_{\underline{b},\underline{x}}(2k^-p_1^+) - 2\,G^{\rm adj}_{\underline{b},\underline{b}'}(2k^-p_1^+)\right)\right] - 2i\,k^i\,\frac{\underline{x}-\underline{b}}{|\underline{x}-\underline{b}|^2}\;\times\;\frac{\underline{y}-\underline{b}}{|\underline{y}-\underline{b}|^2}\,G^{i\,\rm adj}_{\underline{x},\underline{b}}(2k^-p_1^+)\right\}$$

Including small-x evolution

- We need to include small-x evolution on the projectile and target sides.
- This is simple on the target side, less so on the projectile side:

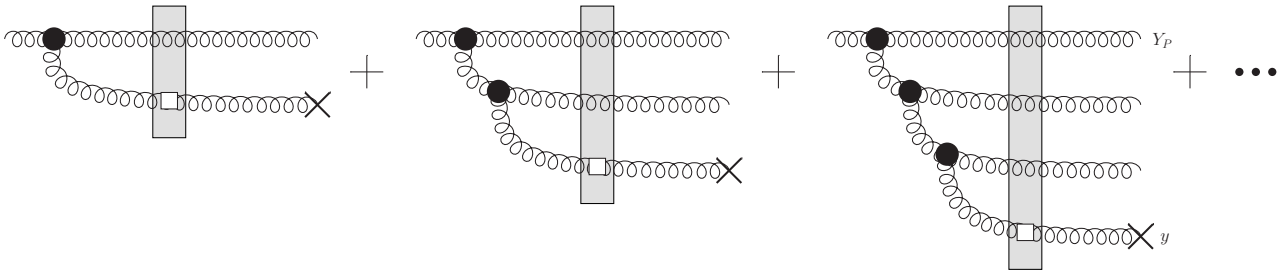

- We symmetrize the above expression with respect to target—projectile interchange, after which we can include the evolution on the projectile side as well.

Gluon production in polarized p+p collisions at mid-rapidity: the final result

- In the end we get the following expression for the cross section (at large N_c), where the dipole amplitudes Q and G_2 evolve via the above evolution equations (YK, M. Li, 2024):

$$\frac{d\sigma}{d^2k_T\,dy} = \frac{C_F}{\alpha_s\,\pi^4}\frac{1}{s\,k_T^2}\int d^2x\, e^{-i\underline{k}\cdot\underline{x}}$$
$$\times \begin{pmatrix} 4\,Q_P & 2\,G_{2P}\end{pmatrix}(x_\perp^2, \sqrt{2}\,p_2^-\,k_T\,e^{-y}) \begin{pmatrix} \frac{1}{4}\overleftarrow{\nabla}_\perp\cdot\vec{\nabla}_\perp & \overleftarrow{\nabla}_\perp{}^2 + \overleftarrow{\nabla}_\perp\cdot\vec{\nabla}_\perp \\ \vec{\nabla}_\perp^2 + \overleftarrow{\nabla}_\perp\cdot\vec{\nabla}_\perp & 0\end{pmatrix}\begin{pmatrix} 4\,Q_T \\ 2\,G_{2T}\end{pmatrix}(x_\perp^2, \sqrt{2}\,p_1^+\,k_T\,e^{y}).$$

- Equivalently, in momentum space we obtain the following factorized expression in terms of TMDs ($\Delta H_{3L}^{\perp}$ is a twist-3 helicity-flip TMD):

$$\frac{d\sigma}{d^2k_T\,dy} = -\frac{32\pi^4\,\alpha_s}{N_c}\frac{1}{s\,k_T^2}\int\frac{d^2q}{(2\pi)^2}$$
$$\times \begin{pmatrix}\Delta H_{3L}^{\perp\,dip\,P} & g_{1L}^{G\,dip\,P}\end{pmatrix}\left(q_T^2, \frac{k_T}{\sqrt{2}\,p_2^-}\,e^{y}\right)\begin{pmatrix}\underline{q}\cdot(\underline{k}-\underline{q}) & \underline{q}\cdot\underline{k} \\ \underline{k}\cdot(\underline{k}-\underline{q}) & 0\end{pmatrix}\begin{pmatrix}\Delta H_{3L}^{\perp\,dip\,T} \\ g_{1L}^{G\,dip\,T}\end{pmatrix}\left((\underline{k}-\underline{q})^2, \frac{k_T}{\sqrt{2}\,p_1^+}\,e^{-y}\right)$$

Polarized p+p collisions: small-x phenomenology

- The above result can be applied to RHIC data
  (D. Adamiak, **N. Baldonado**, et al, 2503.21006 [hep-ph]):

- Note that the calculation was for **gluons only**, quarks need to be included (in progress). Hence, comparison with the data is a proof-of-concept at this point.

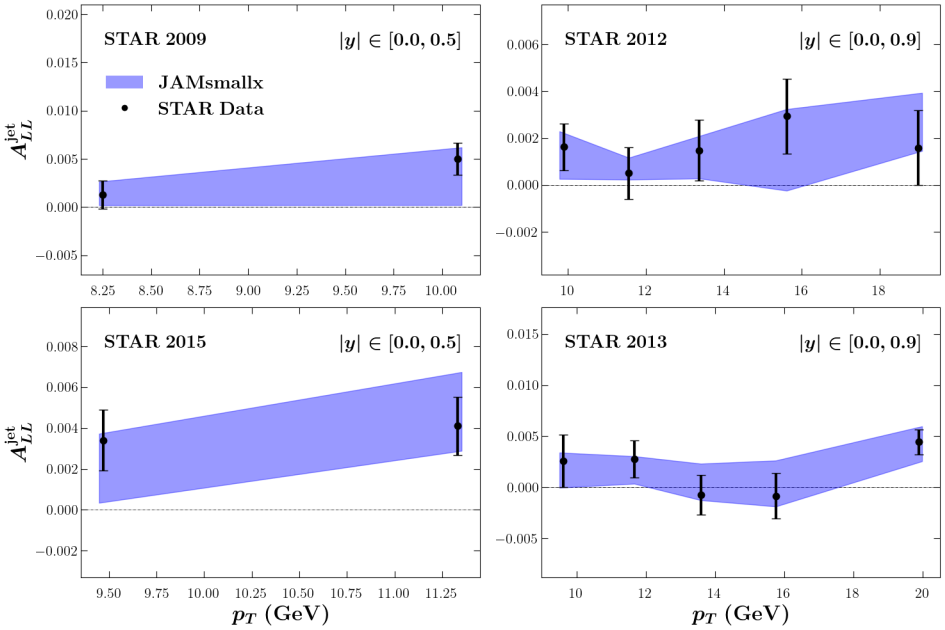

- Only large-N_c evolution (+external quarks) is employed.

Longitudinal Spin: Small-x Evolution

- Small-x evolution can predict helicity distributions at small x.
- **But: hard to fix initial conditions given the existing data** (note: not all polarized p+p data has been analyzed yet).
- End result: also a spread of predictions for EIC.
- EIC will provide constraints:

- Plots are from JAMsmallx, D. Adamiak, **N. Baldonado**, et al, 2503.21006 [hep-ph]

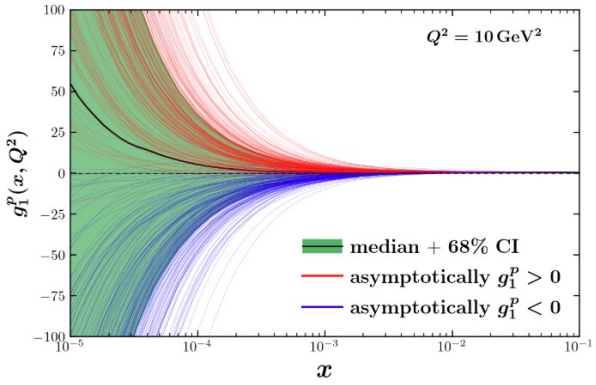

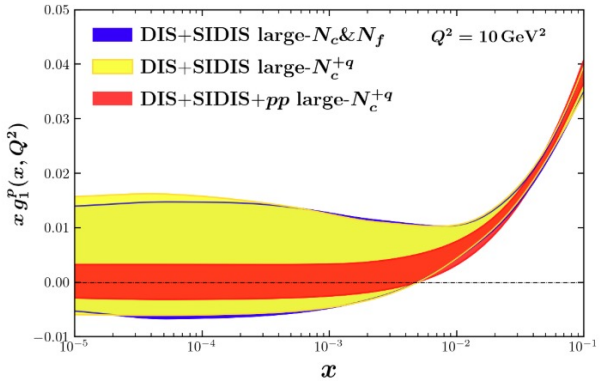

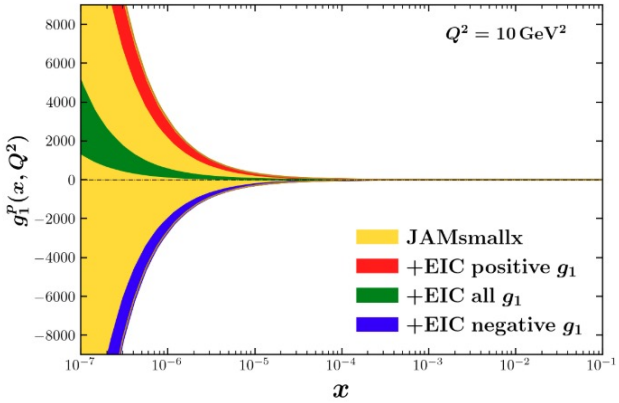

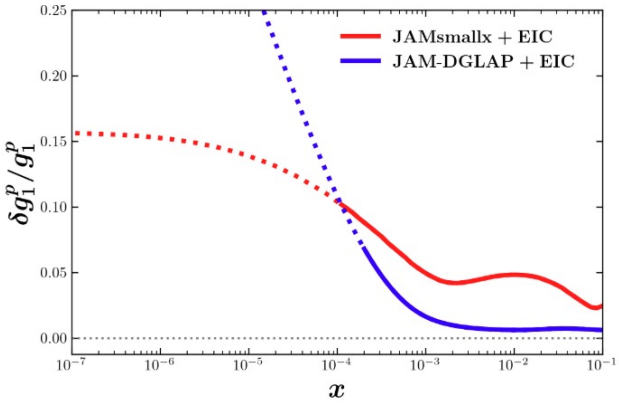

New constraints coming from polarized p+p data:

- Including more data constrains the initial conditions for the dipole amplitudes involved, resulting in more precise EIC predictions for the proton g_1 structure function and estimates of spin at low x:

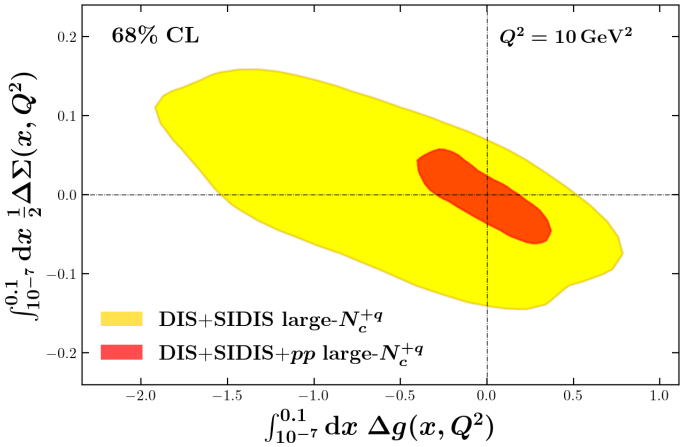

D. Adamiak, **N. Baldonado**, et al, 2503.21006 [hep-ph]

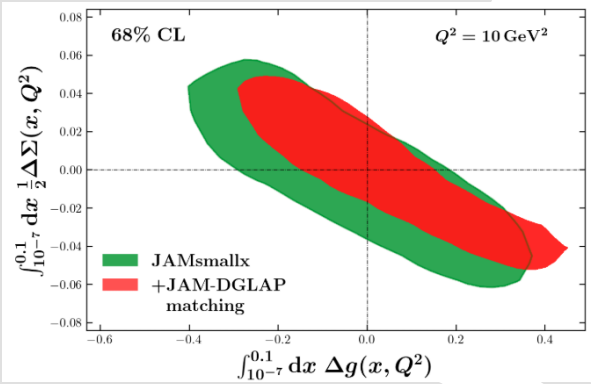

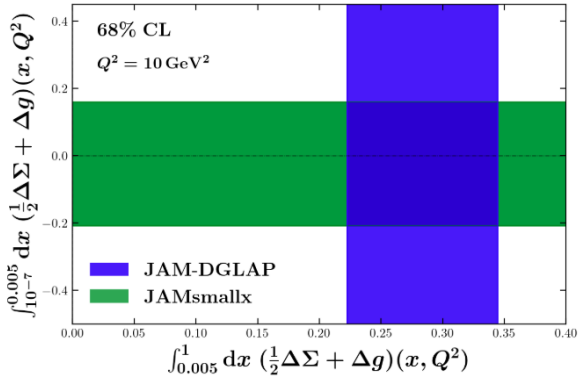

Inclusive dijet production in polarized e+p collisions

YK, M. Li, 2504.12979 [hep-ph]

see Ming's talk

Inclusive dijet production in polarized e+p collisions

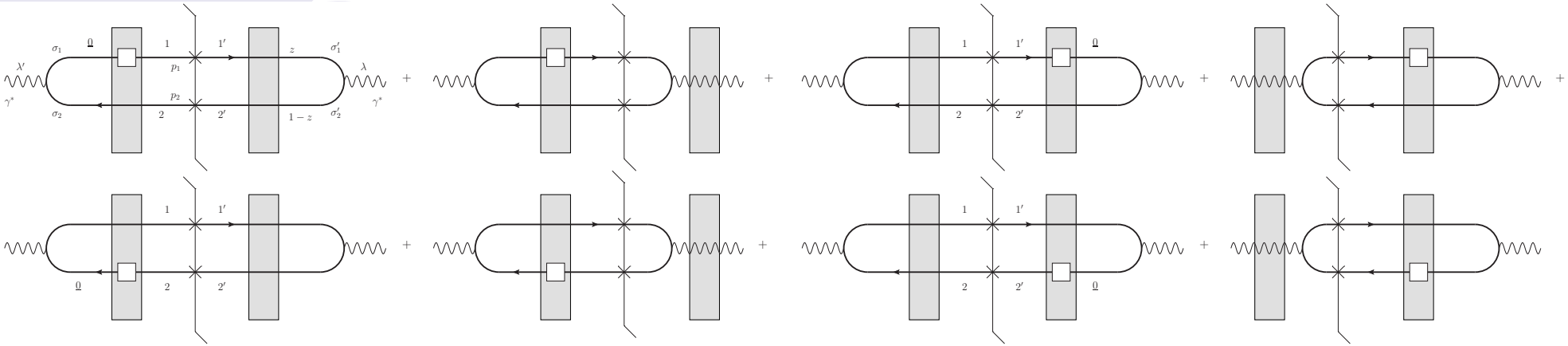

Consider double spin asymmetry (DSA) in inclusive dijet production in e+p collisions. In the b2b limit ($p_T \sim Q >> \Delta_\perp \sim \Lambda_{QCD}$) the cross section probes the WW gluon helicity TMD (cf. F. Dominguez, B.-W. Xiao, and F. Yuan, 2010; F. Dominguez, C. Marquet, B.-W. Xiao, and F. Yuan, 2011, for unpolarized TMDs):

$$\sum_{\lambda=\pm 1} \lambda\, z(1-z)\, \frac{d\sigma_{\lambda\lambda}^{\gamma^* p \to q\bar{q}X}}{d^2p\, d^2\Delta\, dz} \approx -\frac{\alpha_s}{2\pi\, s}\, (eZ_f)^2\, \left[z^2+(1-z)^2\right]\, \frac{p_T^2 - a_f^2}{(p_T^2+a_f^2)^2}\, g_{1L}^{GWW}\left(x \approx \frac{p_T^2}{s}, \Delta_T^2\right)$$

Since, in the linear regime, the two TMDs are the same, $g_{1L}^{GWW}(x,k_T^2) \approx g_{1L}^{G\,dip}(x,k_T^2)$, we can use the future dijet data at EIC to further constrain gluon helicity distribution.

$$a_f^2 = Q^2\, z(1-z) + m_f^2$$

Quark and Gluon OAM at Small x

YK, B. Manley, 2310.18404 [hep-ph]; B. Manley, 2401.05508 [hep-ph];

YK, B. Manley, 2410.21260 [hep-ph].

OAM Distributions

- We begin by writing the (Jaffe-Manohar) quark and gluon OAM in terms of the Wigner distribution as

$$L_z = \int \frac{d^2b_\perp db^- \, d^2k_\perp \, dk^+}{(2\pi)^3} \, (\underline{b} \times \underline{k})_z \, W(k,b)$$

- After much algebra, we arrive at the quark and gluon OAM distributions at small x :

$$\Delta\Sigma(x,Q^2) = \frac{N_f}{\alpha_s \pi^2} \, \widetilde{Q} \left(x_{10}^2 = \frac{1}{Q^2}, s = \frac{Q^2}{x} \right),$$

$$\Delta G(x,Q^2) = \frac{2N_c}{\alpha_s \pi^2} \, G_2 \left(x_{10}^2 = \frac{1}{Q^2}, s = \frac{Q^2}{x} \right),$$

$$L_{q+\bar{q}}(x,Q^2) = -\frac{2\,N_f}{\alpha_s \pi^2} \, \widetilde{I} \left(x_{10}^2 = \frac{1}{Q^2}, s = \frac{Q^2}{x} \right),$$

$$L_G(x,Q^2) = -\frac{2\,N_c}{\alpha_s \pi^2} \left[2\,I_4 + 3\,I_5 \right] \left(x_{10}^2 = \frac{1}{Q^2}, s = \frac{Q^2}{x} \right)$$

OAM Distributions and Moment Amplitudes

$$L_{q+\bar{q}}(x,Q^2) = -\frac{2\,N_f}{\alpha_s \pi^2}\,\widetilde{I}\left(x_{10}^2 = \frac{1}{Q^2}, s = \frac{Q^2}{x}\right),$$

$$L_G(x,Q^2) = -\frac{2\,N_c}{\alpha_s \pi^2}\left[2\,I_4 + 3\,I_5\right]\left(x_{10}^2 = \frac{1}{Q^2}, s = \frac{Q^2}{x}\right)$$

- We now have the impact parameter **moments of dipole amplitudes/operators**:

$$\int d^2x_1\, x_1^m\, \widetilde{Q}_{10}(s) = x_{10}^m\, \widetilde{I}(x_{10}^2, s) + \epsilon^{mi} x_{10}^i\, \widetilde{J}(x_{10}^2, s)$$

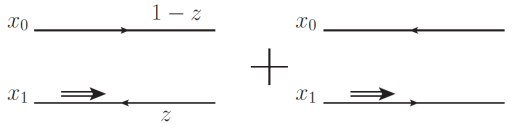

$$\int d^2x_1\, x_1^m\, Q_{10}(s) = x_{10}^m I_3(x_{10}^2, s) + \epsilon^{mj} x_{10}^j J_3(x_{10}^2, s),$$

$$\int d^2x_1\, x_1^m\, G_{10}^i(s) = \epsilon^{mi} x_{10}^2 I_4(x_{10}^2, s) + \epsilon^{mk} x_{10}^k x_{10}^i I_5(x_{10}^2, s) + \delta^{im} x_{10}^2 J_4(x_{10}^2, s) + x_{10}^i x_{10}^m J_5(x_{10}^2, s).$$

Evolution for Moment Dipole Amplitudes

Evolution equations for the moment amplitudes in DLA and at large N_c are derived in YK, B. Manley, 2310.18404 [hep-ph].

They can be solved numerically (same ref) and analytically (B. Manley, 2401.05508 [hep-ph])

$$\begin{pmatrix} I_3 \\ I_4 \\ I_5 \end{pmatrix}(x_{10}^2, zs) = \begin{pmatrix} I_3^{(0)} \\ I_4^{(0)} \\ I_5^{(0)} \end{pmatrix}(x_{10}^2, zs) + \frac{\alpha_s N_c}{4\pi} \int\limits_{\frac{1}{s x_{10}^2}}^{z} \frac{dz'}{z'} \int\limits_{\frac{1}{z's}}^{x_{10}^2} \frac{dx_{21}^2}{x_{21}^2} \begin{pmatrix} 2\Gamma_3 - 4\Gamma_4 + 2\Gamma_5 - 2\Gamma_2 \\ 0 \\ 0 \end{pmatrix}(x_{10}^2, x_{21}^2, z's)$$

$$+ \frac{\alpha_s N_c}{4\pi} \int\limits_{\frac{\Lambda^2}{s}}^{z} \frac{dz'}{z'} \int\limits_{\max[x_{10}^2, \frac{1}{z's}]}^{\min[\frac{z}{z'}x_{10}^2, \frac{1}{\Lambda^2}]} \frac{dx_{21}^2}{x_{21}^2} \begin{pmatrix} 4 & -4 & 2 & -4 & -6 \\ 0 & 4 & 2 & -2 & -3 \\ -2 & 2 & -1 & 4 & 7 \end{pmatrix} \begin{pmatrix} I_3 \\ I_4 \\ I_5 \\ G \\ G_2 \end{pmatrix}(x_{21}^2, z's)$$

$$\begin{pmatrix} \Gamma_3 \\ \Gamma_4 \\ \Gamma_5 \end{pmatrix}(x_{10}^2, x_{21}^2, z's) = \begin{pmatrix} I_3^{(0)} \\ I_4^{(0)} \\ I_5^{(0)} \end{pmatrix}(x_{10}^2, z's)$$

$$+ \frac{\alpha_s N_c}{4\pi} \int\limits_{\frac{1}{s x_{10}^2}}^{z'} \frac{dz''}{z''} \int\limits_{\frac{1}{z''s}}^{\min[x_{10}^2, x_{21}^2 \frac{z'}{z''}]} \frac{dx_{32}^2}{x_{32}^2} \begin{pmatrix} 2\Gamma_3 - 4\Gamma_4 + 2\Gamma_5 - 2\Gamma_2 \\ 0 \\ 0 \end{pmatrix}(x_{10}^2, x_{32}^2, z''s)$$

$$+ \frac{\alpha_s N_c}{4\pi} \int\limits_{\frac{\Lambda^2}{s}}^{z' \frac{x_{21}^2}{x_{10}^2}} \frac{dz''}{z''} \int\limits_{\max[x_{10}^2, \frac{1}{z''s}]}^{\min[\frac{z'}{z''}x_{21}^2, \frac{1}{\Lambda^2}]} \frac{dx_{32}^2}{x_{32}^2} \begin{pmatrix} 4 & -4 & 2 & -4 & -6 \\ 0 & 4 & 2 & -2 & -3 \\ -2 & 2 & -1 & 4 & 7 \end{pmatrix} \begin{pmatrix} I_3 \\ I_4 \\ I_5 \\ G \\ G_2 \end{pmatrix}(x_{32}^2, z''s)$$

Small-x asymptotics of OAM distributions

- Solving the above evolution equations numerically, we arrive at

$$L_{q+\bar{q}}(x,Q^2) \sim L_G(x,Q^2) \sim \left(\frac{1}{x}\right)^{3.66\sqrt{\frac{\alpha_s N_c}{2\pi}}}$$

Consistent with Boussarie, Hatta, Yuan, 2019 (based on BER IREE from 1996) within the numerical precision

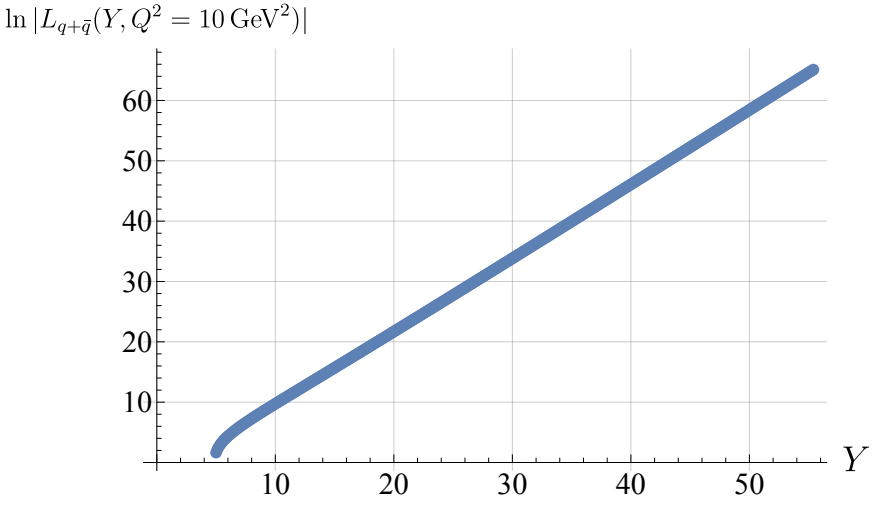

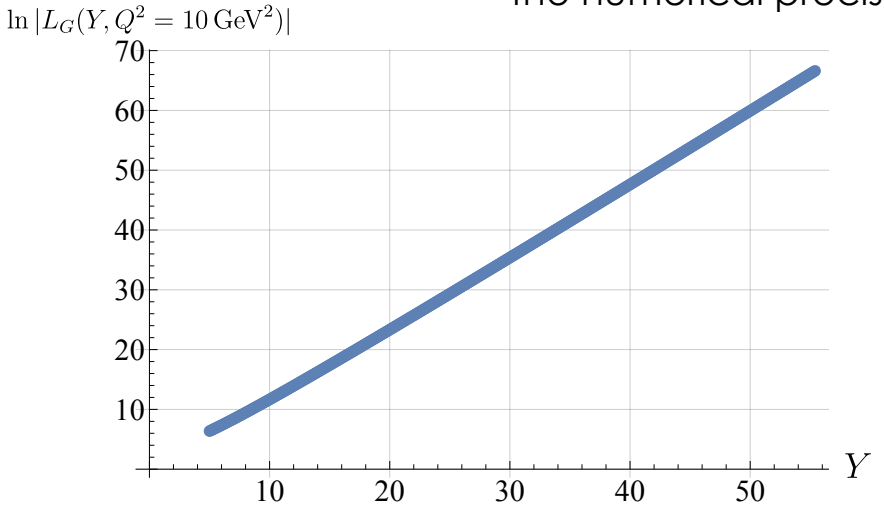

Two intercepts, again

- The evolution equations for moment dipole amplitudes have been solved analytically by B. Manley in 2401.05508 [hep-ph]. The solution was constructed using the double Laplace transform, similar to the solution for the impact-parameter integrated amplitudes.
- The resulting small-x OAM asymptotics at large N_c is the same as for helicity PDFs,

$$L_{q+\bar{q}}(x,Q^2) \sim L_G(x,Q^2) \sim \left(\frac{1}{x}\right)^{\alpha_h}$$

with the intercept

$$\alpha_h = \frac{4}{3^{1/3}} \sqrt{\mathrm{Re}\left[(-9+i\sqrt{111})^{1/3}\right]} \sqrt{\frac{\alpha_s\, N_c}{2\pi}} \approx 3.661 \sqrt{\frac{\alpha_s\, N_c}{2\pi}}$$

- This slightly disagrees with the work of Boussarie, Hatta, and Yuan (2019), which resulted in the same intercept as BER:

$$\alpha_h = \sqrt{\frac{17+\sqrt{97}}{2}} \sqrt{\frac{\alpha_s\, N_c}{2\pi}} \approx 3.664 \sqrt{\frac{\alpha_s\, N_c}{2\pi}}$$

OAM Distribution to hPDF Ratios

- Following Boussarie *et al* (2019), we consider the ratios of OAM distributions to helicity PDFs at small x.
- For these ratios, Boussarie *et al*, predict, inspired by the Wandzura-Wilczek approximation:

$$\frac{L_{q+\bar{q}}(x,Q^2)}{\Delta\Sigma(x,Q^2)} \approx -1 \qquad \frac{L_G(x,Q^2)}{\Delta G(x,Q^2)} \approx -2$$

$$\Delta\Sigma(x,Q^2)\Big|_{x\ll 1} \sim \Delta G(x,Q^2)\Big|_{x\ll 1} \sim \left(\frac{1}{x}\right)^{\alpha_h} \qquad L_{q+\bar{q}}(x,Q^2) \sim L_G(x,Q^2) \sim \left(\frac{1}{x}\right)^{\alpha_h}$$

- Pure WW approximation predicts:

$$\frac{L_{q+\bar{q}}(x,Q^2)}{\Delta\Sigma(x,Q^2)} = -\frac{1}{1+\alpha_h} \qquad \frac{L_G(x,Q^2)}{\Delta G(x,Q^2)} = -\frac{2}{1+\alpha_h}$$

OAM Distribution to hPDF Ratios

- Analytic solution from B. Manley, 2401.05508 [hep-ph], gives

$$t = \sqrt{\frac{\alpha_s\, N_c}{2\pi}\, \ln \frac{Q^2}{\Lambda^2}}$$

$$\alpha_s = 0.25 \qquad \Lambda = 1\ \mathrm{GeV}$$

- Compares well with Boussarie *et al*:

$$\frac{L_{q+\bar{q}}(x,Q^2)}{\Delta\Sigma(x,Q^2)} \approx -1 \qquad \frac{L_G(x,Q^2)}{\Delta G(x,Q^2)} \approx -2$$

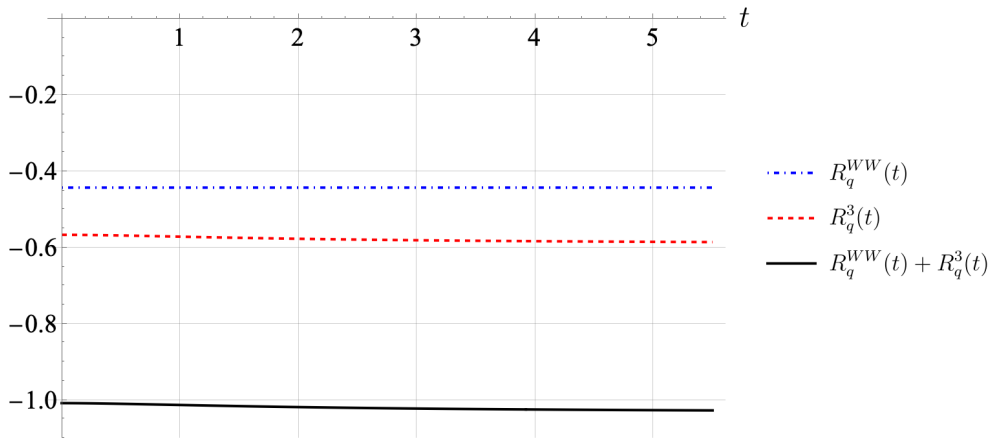

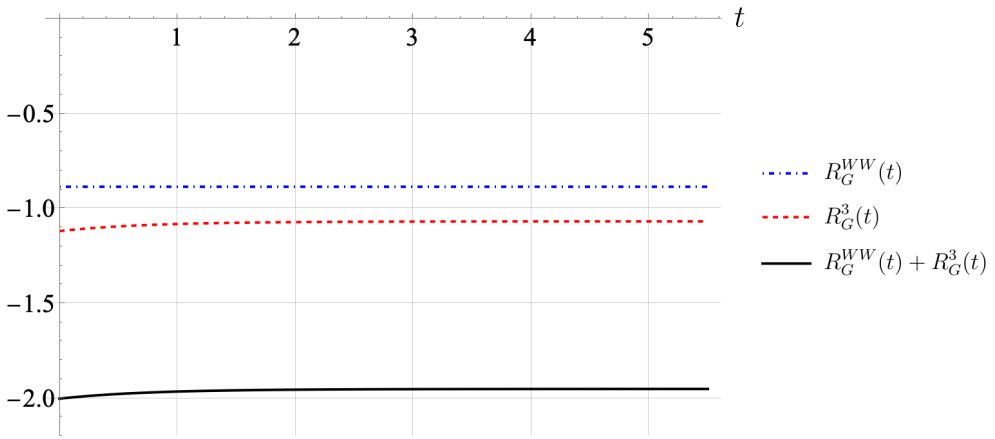

Elastic dijet production in polarized e+p collisions

YK, B. Manley, 2410.21260 [hep-ph]

Elastic dijet production in e+p collisions

The process is similar to the one above, except now the proton remains intact.

One considers two observables, double spin asymmetry (DSA) and single spin asymmetry (SSA):

$$d\sigma^{DSA} = \frac{1}{4} \sum_{\sigma_e, S_L} \sigma_e \, S_L \, d\sigma(\sigma_e, S_L),$$

$$d\sigma^{SSA} = \frac{1}{4} \sum_{\sigma_e, S_L} S_L \, d\sigma(\sigma_e, S_L)$$

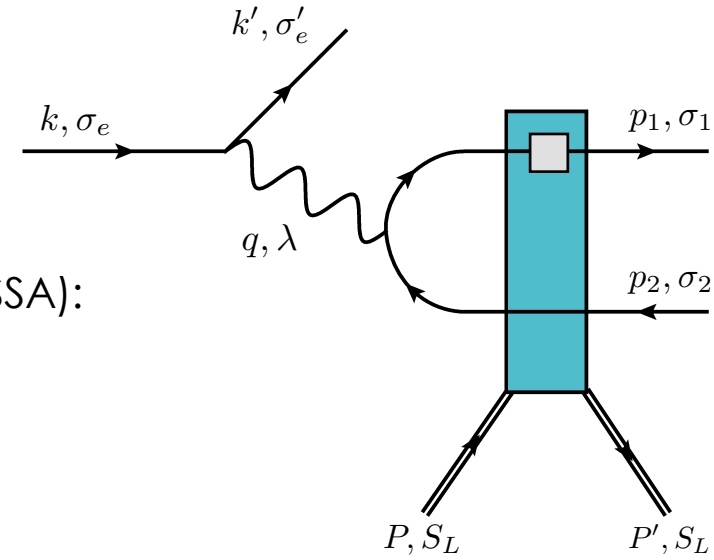

Hatta et al, 2016; S. Bhattacharya, R. Boussarie and Y. Hatta, 2022 & 2024; S. Bhattacharya, D. Zheng and J. Zhou, 2023; YK, B. Manley, 2410.21260 [hep-ph]

Measuring OAM distributions in elastic e+p collisions

- In the small-t limit (pT , Q >> $\Lambda_{QCD} \gg \Delta_\perp$ with $t = -\Delta_\perp^2$) the elastic dijet DSA measures moments of dipole amplitudes I_3, I_4, and I_5, thus **allowing (in principle) to measure OAM distributions!**
- Cf. Hatta et al, 2016; S. Bhattacharya, R. Boussarie and Y. Hatta, 2022 & 2024; S. Bhattacharya, D. Zheng and J. Zhou, 2023.
- Feasibility study in progress (G.Z. Becker, J. Borden, B. Manley, YK).

$$z(1-z)\,\frac{1}{2}\sum_{S_L,\lambda\pm1} S_L\,\lambda\,\frac{d\sigma^{\gamma^* p\to q\bar{q}p'}_{\text{symm. }\lambda\lambda}}{d^2p\,d^2\Delta\,dz} = -\frac{2}{(2\pi)^5 z(1-z)s}\int d^2x_{12}\,d^2x_{1'2'}\,e^{-i\underline{p}\cdot(\underline{x}_{12}-\underline{x}_{1'2'})}\,N(x^2_{1'2'},s) \tag{107a}$$

$$\times\Bigg\{\Bigg[\left(1-2z+i\underline{\Delta}\cdot\underline{x}_{12}\,\left(z^2+(1-z)^2\right)-\frac{i}{2}\underline{\Delta}\cdot\underline{x}_{1'2'}\,(1-2z)^2\right)Q(x^2_{12},s)-i\underline{\Delta}\cdot\underline{x}_{12}\,I_3(x^2_{12},s)$$

$$-i\underline{\Delta}\times\underline{x}_{12}\,J_3(x^2_{12},s)\Bigg]\Phi^{[1]}_{\text{TT}}(\underline{x}_{12},\underline{x}_{1'2'},z)$$

$$+\Bigg[i(1-2z)\Big(\Delta^j\epsilon^{ji}x^2_{12}I_4(x^2_{12},s)+\underline{\Delta}\times\underline{x}_{12}\,x^i_{12}I_5(x^2_{12},s)+\Delta^i\,x^2_{12}J_4(x^2_{12},s)+\underline{\Delta}\cdot\underline{x}_{12}\,x^i_{12}J_5(x^2_{12},s)\Big)$$

$$-\left[1+i\,(1-2\,z)\,\underline{\Delta}\cdot\left(\underline{x}_{12}-\frac{\underline{x}_{1'2'}}{2}\right)\right]\left(\epsilon^{ik}x^k_{12}G_2(x^2_{12},s)+x^i_{12}G_1(x^2_{12},s)\right)\Bigg]$$

$$\times\left(\partial^i_\perp-ip^i\right)\Phi^{[2]}_{\text{TT}}(\underline{x}_{12},\underline{x}_{1'2'},z)\Bigg\}+\mathcal{O}(\Delta^2_\perp),$$

$$z(1-z)\,\frac{1}{2}\sum_{S_L,\lambda=\pm1} S_L\left[e^{i\lambda\phi}\,\frac{d\sigma^{\gamma^* p\to q\bar{q}p'}_{\text{symm. }0\lambda}}{d^2p\,d^2\Delta\,dz}+\text{c.c.}\right] = -\frac{2i\sqrt{2}}{2(2\pi)^5 z(1-z)s}\int d^2x_{12}\,d^2x_{1'2'}\,e^{-i\underline{p}\cdot(\underline{x}_{12}-\underline{x}_{1'2'})} \tag{107b}$$

$$\times N(x^2_{1'2'},s)\Bigg\{\Bigg[\left(1-2z+i\,\underline{\Delta}\cdot\underline{x}_{12}\,\left(z^2+(1-z)^2\right)-\frac{i}{2}\underline{\Delta}\cdot\underline{x}_{1'2'}\,(1-2z)^2\right)Q(x^2_{12},s)-i\underline{\Delta}\cdot\underline{x}_{12}\,I_3(x^2_{12},s)$$

$$-i\underline{\Delta}\times\underline{x}_{12}\,J_3(x^2_{12},s)\Bigg]\left[\frac{\hat{k}\cdot\underline{x}_{12}}{x_{12}}\Phi^{[1]}_{\text{LT}}(\underline{x}_{12},\underline{x}_{1'2'},z)-\frac{\hat{k}\cdot\underline{x}_{1'2'}}{x_{1'2'}}\Phi^{[1]}_{\text{LT}}(\underline{x}_{1'2'},\underline{x}_{12},z)\right]$$

$$+\Bigg[i(1-2z)\Big(\Delta^j\epsilon^{ji}\,x^2_{12}\,I_4(x^2_{12},s)+\underline{\Delta}\times\underline{x}_{12}\,x^i_{12}\,I_5(x^2_{12},s)+\Delta^i\,x^2_{12}\,J_4(x^2_{12},s)+\underline{\Delta}\cdot\underline{x}_{12}\,x^i_{12}\,J_5(x^2_{12},s)\Big)$$

$$-\left[1+i\,(1-2\,z)\,\underline{\Delta}\cdot\left(\underline{x}_{12}-\frac{\underline{x}_{1'2'}}{2}\right)\right]\left(\epsilon^{ik}x^k_{12}G_2(x^2_{12},s)+x^i_{12}G_1(x^2_{12},s)\right)\Bigg]$$

$$\times\left(\partial^i_\perp-ip^i\right)\left[\frac{\hat{k}\times\underline{x}_{12}}{x_{12}}\Phi^{[2]}_{\text{LT}}(\underline{x}_{12},\underline{x}_{1'2'},z)+\frac{\hat{k}\times\underline{x}_{1'2'}}{x_{1'2'}}\Phi^{[2]}_{\text{LT}}(\underline{x}_{1'2'},\underline{x}_{12},z)\right]\Bigg\}+\mathcal{O}(\Delta^2_\perp),$$

OAM measurement with elastic dijets: feasibility study (very preliminary!)

Vertical axis – cos $\phi_{\Delta pT}$ harmonic in elastic dijets A_{LL}.

pT = jets b2b momentum
Δ = momentum transfer
assumed int. luminosity = 100 fb^{-1}

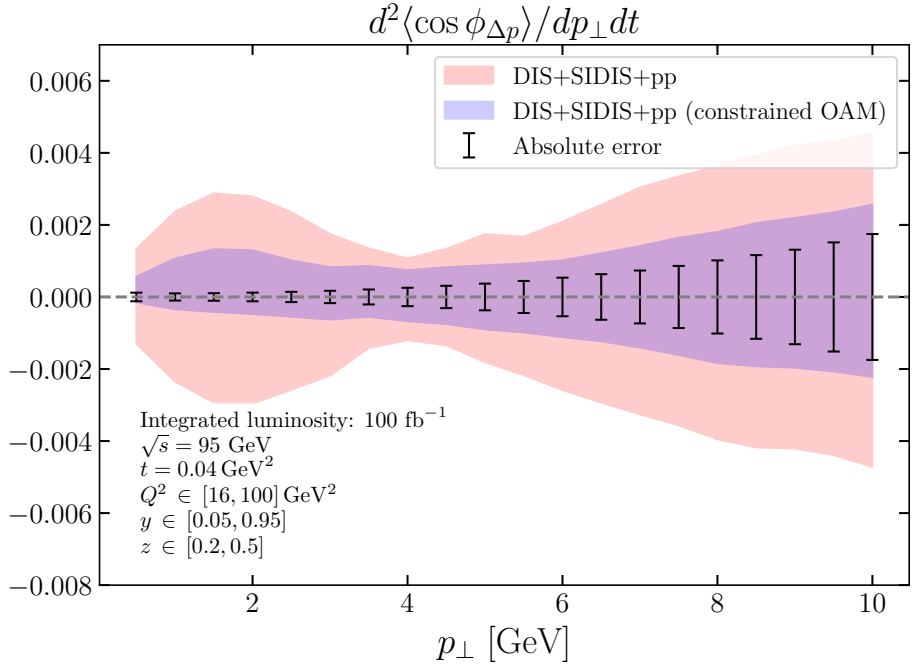

JAMsmallx (Brandon Manley) – **preliminary!**

Conclusions

- The small-x helicity formalism in the double logarithmic approximation (DLA) + running coupling allows to do successful polarized DIS + SIDIS phenomenology based on the existing small-x data.
- However, the multitude of different dipole amplitudes in the formalism prevents precise EIC predictions: there are too many initial conditions to fix using the existing data.
- Polarized p+p data on A_{LL} from RHIC, if properly included, may help. The first step in this direction was presented above.
- When EIC comes online, DSA in inclusive dijet production will help constrain gluon helicity distributions.
- Elastic dijets at EIC may help us measure the OAM distributions as well (and compare their x-dependence to theory).